SCIENTIA AGROPECUARIA

Scientia Agropecuaria

Web page: http://revistas.unitru.edu.pe/index.php/scientiaagrop

Facultad de Ciencias Agropecuarias

Universidad Nacional de Trujillo

RESEARCH ARTICLE

Groundwater quality and irrigation suitability assessment in a semi-arid agricultural aquifer of northern Peru

Harold Ore-Quiroz[1]*; Carlos Salazar-Sandoval[1]; Ericka Olaya-Ato[1], Lizbeth Camacho-Vidal[1]; Lesly Espinoza-Haro[2]

[1] Escuela Profesional de Ingeniería en Industrias Alimentarias, Universidad Nacional de Frontera, Sullana, Piura, Peru.
[2] Escuela Profesional de Ingeniería en Ingeniería Agroindustrial, Universidad Nacional del Santa, Chimbote, Ancash, Peru.

* Corresponding author: hore@unf.edu.pe (H. Ore-Quiroz).

Received: 31 March 2026. Accepted: 12 October 2026. Published: 22 October 2026.

Abstract

In semi-arid coastal regions, groundwater mineralization limits water-usage opportunities because of the intersection of natural hydrogeochemical processes with agricultural and urban pressures. The present study analyzed groundwater quality in 25 wells of the Sullana aquifer in northern Peru, within the context of a dry-season campaign. Physicochemical characterization incorporated ionic ratios, the cationic Gibbs relationship, principal component analysis, hierarchical cluster analysis, a weighted arithmetic Water Quality Index, irrigation indicators, and spatial analysis on GIS. Results of our study showed the electric conductivity in the range of 656 - 17290 µS/cm and total chloride amounts of up to 4522.60 mg/L. Comparison data on the electric conductivity showed exceedance for 44% of wells, 40% for total dissolved solids, 88% for chloride levels, and 56% for sulfate levels. The total variance is accounted for by two primary components at 78.46%, where major-ion mineralization is demarcated from Fe–Mn variability. The Water Quality Index labels some 84% of wells either poorly, very poorly, or unsuitable for drinking water due to untreated conditions. Manganese was present in three wells at over 0.40 mg/L, while certain As, Pb, Cd, and Cu findings remain uncertain and need confirmation through calculations based on laboratory reporting parameters, detection parameters, and quantification parameters, Major-ion mineralization and localized manganese accumulation remained as the two main issues regarding the quality of groundwater, causing the necessity for seasonal tracking, hydro-geological monitoring, and more hydrochemical analysis or isotopic tracing for better understanding of salinity origins and leading the way to sustainable extraction of ground waters in the future.

Keywords: Groundwater mineralization; ionic ratios; Water Quality Index; multivariate analysis; manganese; irrigation suitability; semi-arid aquifer; Sullana.

DOI: https://doi.org/10.17268/sci.agropecu.2026.061

Cite this article:

Ore-Quiroz, H., Salazar-Sandoval, C., Olaya-Ato, E., Camacho-Vidal, L., & Espinoza-Haro, L. (2026). Groundwater quality and irrigation suitability assessment in a semi-arid agricultural aquifer of northern Peru. *Scientia Agropecuaria, 17*(4), 921-942.

1. Introduction

Groundwater is essential for drinking water supply, agriculture irrigation, and socioeconomic development, especially in dry and semi-dry areas with poor and irregular surface water resources. The composition of groundwater is a result of some natural and anthropogenic processes such as mineral dissolution, ion exchange, redox processes, evaporation, and water-rock interaction along with the hydraulic pressure resulting from agriculture, wastewater infiltration, urbanization, and overutilization of groundwater (Appelo & Postma, 2005; Mukherjee & Singh, 2022; Wang et al., 2026). In coastal aquifers irrigation return flow, saltwater mixing, and seawater intrusion may additionally influence the composition of major ions and mobility of trace metals (Slama et al., 2022).

Thus, an integrated assessment is needed to differentiate the overlapping processes involved. Physicochemical parameters and major ions are useful for tracing mineralization patterns and hydrochemical evolution, while trace-element analysis establishes whether groundwater contamination involves toxic elements as well. By employing multivariate statistical and clustering methods, it becomes possible to determine the relationship between the parameters concerned and identify wells with similar chemical compositions. When GIS is integrated with statistical techniques, the resulting approach becomes a useful tool for mapping spatial variations in chemical composition and areas of interest for further monitoring. It is also important to note that statistical categorizations and interpolation do not enable the identification of pollution sources, water

flow paths, and connectivity of aquifers (Narvaez-Montoya et al., 2024; Tziritis et al., 2024).

Research on aquifers in semi-arid regions along the coast suggests that groundwater that is rich in Na-Cl and sulfate ions may come about due to processes like evaporation, evaporite dissolution, ion exchange, irrigation, residual salinity, or recent saline water intrusion (El Mountassir & Bahir, 2023; Ji et al., 2024; Wurl et al., 2023). This means that salinity and trace elements should be assessed separately as salinity does influence the mobility of metals, but the behaviour of trace elements is determined by pH, redox conditions, mineral surfaces, the presence of organic matters, and formation of complexes (Zhi et al., 2022).

The integration of well-scale data from north Peru seems to be scarce. Assessment of the region of the Chira-Piura basin takes into account irrigation, salinity and drainage issues, pollution, climatic changes, availability of data on groundwater without any clear patterns but does not provide sufficient information about the changes in hydrochemistry of separate wells located in Sullana (Consorcio ATA–UNP–UNL, 2005; Autoridad Nacional del Agua (ANA), 2015).

In this research, physicochemical factors, principal ions, trace elements, ionic ratios, multivariate statistics, measures of drinking and irrigation water, and GIS-based spatial analysis are combined. The objective of this research is the description of groundwater chemistry, determining dominant hydrochemical associations, assessment of restrictions of groundwater use for drinking and irrigation purposes, and defining priority monitoring zones. The dry season baseline obtained provides support for groundwater quality management in addition to identification of information which should be collected for subsequent studies on salinity sources discrimination.

2. Methodology

2.1. Study area

2.1.1. Geographic setting

The study was performed in the Sullana aquifer located in the lower basin of the Chira River within Piura Region in northern Peru (Figure 1). It is a part of the Chira Valley which is a part of the aquifer system of the Catamayo–Chira basin on a binational scale. The Chira basin covers 17,199.18 km², out of which Peru accounts for 9,986.81 km² and Ecuador 7,212.37 km². The basin spreads over the Pacific coast up to the height of 3,700 meters in the Andes mountain range. The current research work describes the aquifer system present around Sullana (Consorcio ATA–UNP–UNL, 2005; ANA, 2015). The Catamayo–Chira River serves as the major drainage system of the region and runs around 315 km between the Andes and the Pacific Ocean. Its mean discharge is about 98.85 m^3/s. However, flow of the river varies significantly depending on weather, seasonal rainfall, water requirements, and reservoir operation (Consorcio ATA–UNP–UNL, 2005; ANA, 2015).

The Poechos Reservoir, the Sullana Diversion Dam, and the related irrigation system exert a huge impact on regional hydrology. Thus, such hydraulic projects control the storage and distribution of surface water and may indirectly affect the groundwater recharge and quality due to river-aquifer transfer, canal leakage, return irrigation flow, agricultural drainage, and water withdrawal (ANA, 2015; Proyecto Especial Chira Piura [PECHP], 2021). The studied region combines agriculture, urbanization, and peri-urbanization, as groundwater is supplemental to surface water for domestic, agricultural, and industrial purposes.

2.1.2. Climatic characteristics

Characterized by a warm, semi-arid climate, the lower Chira Valley experiences an average temperature of about 24 °C. Rainfall is concentrated from January to April in a normal year, where it typically ranges from 10 to 80 mm $year^{-1}$, while the evaporation rate can reach an average of 6 mm day^{-1}. The continuous water deficit in this region promotes evaporative concentration.

The El Niño–Southern Oscillation disturbs this climatological state every so often, specifically the coastal El Niño which can lead to rainfall, floods, and ground water level increase, thereby increasing recharge, drainage, and sediment transport (ANA, 2015). In this way, aquifer recharge becomes episodic and varies widely in terms of space. Periods of excessive rain favor water infiltration leading to dissolution of substances; prolonged dry periods, on the contrary, do not allow essential aquifer flushing to occur leading to problems with solute accumulation at the site (Consorcio ATA–UNP–UNL, 2005; ANA, 2015).

Since groundwater was sampled only once during the dry season, the findings reflect the situation during that specific sampling campaign and cannot indicate any seasonal variations or long-term trends. Consequently, it is essential to repeat the sampling of groundwater during wet and dry seasons for the analysis of water dilution, evaporation, and temporal modifications in the groundwater quality level.

2.1.3. Geological and hydrogeological framework

The Sullana aquifer is largely formed within Quaternary fluvial and alluvial deposits of the lower Chira Valley. Loose gravel and sand are the main groundwater storing and transferring areas, while silt and clay lenses can sometimes stop vertical flow progression. Nonetheless, the evidence available does not indicate that confined or semi-confined aquifer layers are distributed all over the system.

Groundwater exists mainly under the unconfined state. The sediment structure of the region, its thickness, leakage from the Chira River, seepage from canals, its irrigation methods, and the presence of sandy formations affect its hydrodynamic behavior. There were no measurements of transmissivity, the storage coefficient, vertical hydraulic gradients, screen intervals, and the connections between shallow and deep formations. As a result, it is impossible to develop a definite picture of the flow of groundwater or define the vertical hydrochemical relationships.

It has been evaluated that there are 250 hm^3 of groundwater resources in the Chira alluvial aquifer. Nevertheless, this evaluation only portrays general estimates, so the regional amount may not reflect groundwater storage and recharge in the 25 wells sampled (ANA, 2015). Recharge processes may involve water being lost from the Chira River, seepage from canals, irrigation return flows, rainwater infiltration, and inflow of water tables. On the other hand, groundwater may be removed by pumping, evapotranspiration, agricultural drainage and river-aquifer interchange processes (Consorcio ATA–UNP–UNL, 2005; ANA, 2015).

Shallow groundwater levels, poor drainage, and high electrical conductivity have been discussed in historical evaluations, suggesting a possibility of salinization issues. However, these elements do not prove seawater intrusion by themselves (Consorcio ATA-UNP-UNL, 2005). Thus, hydrochemical phenomena were interpreted based on the data of groundwater obtained within the current project rather than through the knowledge of geological and hydrogeological conditions in the specific region.

2.1.4. Land use and potential contamination sources

The land use of Sullana consists of agricultural practice, cities, pastureland, transportation facilities as well as businesses. About 40.63% of the whole Catamayo–Chira region consists of forests, while pasture, shrubland, arable land, and Andean ecosystems cover the rest. However, the figures for the basin as a whole do not reflect how land is used in the area of this study, where agriculture and urban land use are more widely practiced (Consorcio ATA–UNP–UNL, 2005).

Water requirements from agricultural practices and livestock production constitute approximately 94.04% of total water consumption in the basin and involve almost 64,900 hectares of irrigated area. Under conditions of high evaporation rates, a shallow groundwater table, ineffective irrigation and poor drainage systems, irrigation return flows can bring along dissolved salts, nutrients and agricultural chemicals into shallow groundwater (Consorcio ATA–UNP–UNL, 2005).

Urbanization in Sullana and Bellavista is exerting additional stress owing to the presence of wastewater discharges, malfunctioning sewerage systems, sewerage treatment plants, solid waste leachate, and stormwater run-off (ANA, 2015). The use of animal waste and agricultural drainage could also result in the addition of salts, nutrients and microbial contamination where infiltration pathways exist. All the interactions were deemed context pressure and not confirmed contamination sources. The proximity of the well to a certain land use was not interpreted as evidence of a causal relationship. Source attribution cannot take place without groundwater flow data and other indicators.

2.1.5. Groundwater sampling network

The process of selecting operational groundwater wells (M1–M25) was done according to a purpose-oriented method to cover the area of the Sullana aquifer under study. While selecting the wells for study, various factors, such as easy approach to wells, their operational status, land use methods in the vicinity, closeness to the Chira River and irrigation system, and geographical location of agricultural, urban & different hydrochemical zones were taken into consideration.

This network provides a foundation for discovering patterns in groundwater quality and for comparison between different sections that have been monitored so far. Nevertheless, because the chosen wells were selected based on their availability and accessibility, it cannot be regarded as a fully randomized or representative network of aquifers.

Each well was sampled one time per dry-season campaign so only spatial comparisons can be made using the dataset without any correlation to seasonal fluctuations, dilution of water since its recharge or long-term groundwater quality observations. Re-sampling of the wells during wet and dry seasons along with measurements of the water table would be necessary to determine any changes over time in regard to recharge, mineralization processes and water quality.

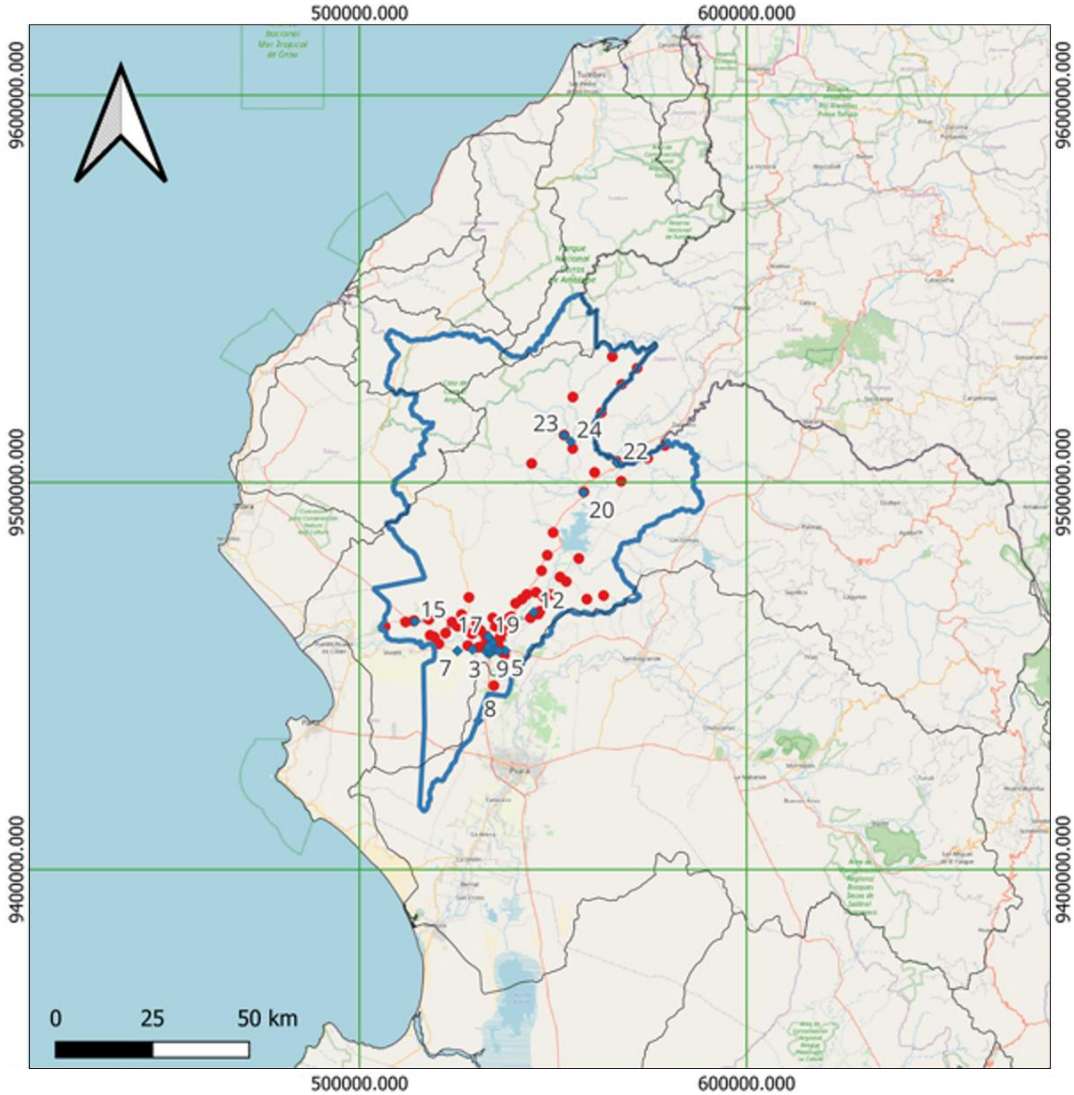


Figure 1. Location of the domain of the Chira groundwater study and spatial distribution of the 25 groundwater sampling sites. Note. Red symbols show wells M1–M25; the blue outline marks the study domain. Coordinates use UTM zone 17M. Symbols indicate sampling locations, not contamination, recharge, vulnerability, or regulatory exceedances.

2.2. Sampling design and well characterization

A purposive network of 25 operational groundwater wells (M1–M25) was established within the sampled sector of the Sullana aquifer. Well selection considered accessibility, operational status, reported depth, surrounding land use, and spatial distribution. Because the network depended on the availability and accessibility of operational wells, it provides an exploratory hydrochemical baseline rather than a randomized or exhaustive representation of the aquifer. Uneven spatial coverage was therefore considered when interpreting groundwater-quality patterns (Ohmer et al., 2019).

Well locations were verified using Google Earth Pro and recorded in UTM zone 17M. Reported total well depths ranged from 10 to 93 m (Table 1). Because screened intervals and pump-intake depths were unavailable, chemical differences among wells were not interpreted as evidence of vertical hydrochemical stratification.

The 25 wells represented 24 unique horizontal locations because M2 and M3 shared the same coordinates but had different reported total depths. Both wells were retained as independent observations in the descriptive and multivariate analyses. For two-dimensional IDW interpolation, their parameter-specific arithmetic mean was used at the shared coordinate to avoid duplicating a spatial location.

Groundwater sampling was conducted during a single dry-season campaign. Before sample collection and field measurements, each operational well was pumped until the measured field parameters stabilized, following ISO 5667-11:2009 (ISO, 2009).

Table 1
Geographic coordinates and reported total depths of the groundwater sampling wells

Sample code	Reported depth (m)	UTM zone	Easting (m E)	Northing (m N)
M1-1124/PHCS	20	17M	533,592	9,455,746
M2-1124/PPJP1	50	17M	532,832	9,456,179
M3-1124/PLP2	90	17M	532,832	9,456,179
M4-1124/PF	30	17M	532,777	9,456,222
M5-1125/PJE	35	17M	537,737	9,456,502
M6-1126/PV1	42	17M	525,347	9,456,446
M7-1126/PV2	25	17M	525,348	9,456,450
M8-1126/PT	35	17M	530,754	9,438,464
M9-1127/PS1	40	17M	533,906	9,456,228
M10-1127/PZ/S2	25	17M	533,869	9,456,267
M11-1128/PA	10	17M	534,959	9,456,672
M12-1129/PM	93	17M	545,032	9,466,464
M13-1129/PPR	15	17M	534,369	9,458,644
M14-1129/PLV	25	17M	535,983	9,456,452
M15-1129/PSF	20	17M	514,329	9,464,062
M16-1130/PO	30	17M	529,205	9,456,783
M17-1130/PM1	35	17M	533,355	9,460,137
M18-1130/PCH	15	17M	533,233	9,457,454
M19-1130/PM2	35	17M	533,314	9,460,110
M20-1201/PLV	28	17M	557,854	9,497,342
M21-1201/PLM	46	17M	557,864	9,497,382
M22-1201/PLA	32	17M	566,597	9,504,959
M23-1202/PLQS	45	17M	552,932	9,512,136
M24-1202/PLJN	15	17M	554,645	9,510,508
M25-1202/PLJN	10	17M	529,777	9,457,273

Note. Coordinates are reported in UTM zone 17M, as recorded in the original field database. Easting and northing values are expressed in meters.

2.3. Field measurements and instrumentation

In situ measurements at each well were obtained using an HI98194 portable multiparameter meter equipped with an HI7698194 digital multisensor probe (Hanna Instruments, Woonsocket, RI, USA). The recorded parameters included water temperature, pH, electrical conductivity (EC), total dissolved solids (TDS), and dissolved oxygen (DO). Further technical specifications for the meter and probe are provided in Table 2. The probe included a combined pH/ORP sensor, a four-ring conductivity sensor, a galvanic DO sensor, and an integrated temperature sensor. Automatic temperature compensation was applied to the corresponding measurements. TDS was calculated from EC using the conversion factor configured in the instrument and was therefore treated as an EC-derived parameter rather than an independent gravimetric measurement.

Before each sampling session, the probe was inspected and calibrated according to the manufacturer's instructions. Calibration status and electrode performance were documented using the instrument's Good Laboratory Practice function. Each well was pumped before measurements to displace standing water from the casing and delivery system. Readings were obtained from freshly pumped groundwater while minimizing aeration, agitation, heating, and measurement delays. Final values were recorded after the field parameters had stabilized, following ISO 5667-11:2009 (ISO, 2009). ORP and barometric pressure are reported in Table 2 as instrument capabilities. They should be treated as study variables only if the corresponding field readings and calibration records are available.

2.4. Sample collection, preservation, and transport

Groundwater samples were collected after well purging and stabilization of the field parameters. Water was transferred directly into pre-cleaned high-density polyethylene bottles while minimizing aeration, sample disturbance, and external contamination. Each container was labeled with the well code, collection date and time, analytical fraction, and preservation treatment. Sample collection, preservation, and handling followed ISO 5667-3:2024 and Standard Methods for the Examination of Water and Wastewater, 24th edition (ISO, 2024; Lipps et al., 2023).

Separate aliquots were prepared for major-ion and dissolved-element analyses. Samples intended for major-ion determination were not acidified. Samples for dissolved-element analysis were filtered through 0.45-µm membrane filters, transferred into acid-cleaned bottles, and preserved with ultrapure nitric acid to pH < 2. Elemental results therefore represented the operationally defined dissolved fraction.

Samples were enclosed, shielded from light, kept upright in insulated boxes at around 4 °C and taken to the lab in accordance with holding time requirements. Chain-of-custody protocols recorded sam-

ple identification, as well as its collection and receiving times, preservation methods, transportation conditions, requested analysis, as well as any deviation from established procedures. Samples that suffered from leakage, receiving incompletely labeled, improperly preserved, or inappropriately transported conditions were examined before accepting them in the validated dataset.

2.5. Laboratory analytical methods

Groundwater samples were analyzed for total hardness, chloride, sulfate, and trace elements using the equipment summarized in Table 3. Spectrophotometric determinations were performed with a UV5 UV–Vis spectrophotometer (METTLER TOLEDO, Switzerland), while analyses requiring graphite-furnace atomic absorption spectrometry were conducted using an AA-7000 instrument (Shimadzu, Japan). Multielement analysis was carried out with a NexION 2000 inductively coupled plasma mass spectrometer (PerkinElmer, USA).

The analytical program included Ag, Al, As, B, Ba, Be, Ca, Cd, Ce, Co, Cr, Cu, Fe, Hg, K, Li, Mg, Mn, Mo, Na, Ni, P, Pb, Sb, Se, SiO_2, Sn, Sr, Ti, Tl, V, Zn, and S. Traceable calibration standards and internal standards were used to monitor instrumental drift and matrix effects. Validated collision or reaction modes were applied when needed to minimize spectral interferences.

When digestion was required, samples were processed in closed vessels using an ETHOS UP microwave digestion system (Milestone, Italy). Total hardness, chloride, and sulfate were determined using the corresponding validated laboratory procedures. Analyte-specific calibration ranges, limits of detection (LOD), limits of quantification (LOQ), and reporting limits were established according to the applicable analytical methods (Cantwell, 2025). Results below the reporting limit were treated as censored observations because analytical sensitivity depends on the instrument, calibration procedure, sample matrix, spectral interferences, and formal method validation.

Table 2
Operating characteristics of the field multiparameter meter

Parameter	Sensor or calculation	Measurement range	Resolution	Manufacturer-reported accuracy	Calibration
pH	HI7698194-1 combined pH/ORP sensor	0.00–14.00	0.01	±0.02 pH units	Automatic, up to three points
ORP	Platinum pin in HI7698194-1 sensor	±2,000.0 mV	0.1 mV	±1.0 mV	One custom point
EC	HI7698194-3 four-ring conductivity sensor	0–200 mS cm^{-1}; absolute EC up to 400 mS cm^{-1}	1 µS cm^{-1} within 0–9,999 µS cm^{-1}	±1% of reading or ±1 µS cm^{-1}	One point using certified EC standard
TDS	Calculated from EC using selected TDS factor	0–400,000 mg L^{-1}	1 mg L^{-1} within 0–9,999 mg L^{-1}	±1% of reading or ±1 mg L^{-1}	Based on EC calibration
DO	HI7698194-2 galvanic DO sensor	0.00–50.00 mg L^{-1}; 0.0–500.0%	0.01 mg L^{-1}; 0.1%	Range-dependent	Automatic, one or two points
Temperature	Integrated temperature sensor	−5.00–55.00 °C	0.01 °C	±0.15 °C	One custom point
Barometric pressure	Integrated barometer	450–850 mm Hg	0.1 mm Hg	±3 mm Hg	One custom point

Note. Measurements used an HI98194 meter with an HI7698194 probe. TDS was EC-derived. ORP and pressure should be reported only when recorded in the field. Instrument specifications were manufacturer-provided directly.

Table 3
Laboratory instruments and analytical applications

Equipment	Manufacturer and model	Analytical application	Information required in the final method
UV-Vis spectrophotometer	METTLER TOLEDO UV5	Spectrophotometric determination of documented water-quality parameters	Analytes, wavelength, reagent method, calibration range, LOD, LOQ
Graphite-furnace atomic absorption spectrophotometer	Shimadzu AA-7000	Trace-element determination according to the laboratory method	Elements, wavelength, lamp, furnace program, matrix modifier, LOD, LOQ
Inductively coupled plasma mass spectrometer	PerkinElmer NexION 2000	Multielement determination of trace elements	Isotopes, internal standards, cell mode and gas, calibration range, LOD, LOQ
High-pressure microwave digestion system	Milestone ETHOS UP	Acid digestion of analytical fractions requiring decomposition	Sample volume, acid mixture, temperature, ramp, holding time, final volume

Note. The table lists verified equipment. Capabilities do not confirm analyses. Analyte assignments require reports, calibration records, and methods; manufacturer specifications are not detection limits.

2.6. Quality assurance and quality control (QA/QC)

Quality assurance and quality control covered sample collection, handling, and laboratory analysis. The processes have blanks, duplicate samples, analytical replicates, retained disks, calibration verification, and limits of detection of each analyte. Blanks help to determine contamination, duplicate samples determine accuracy, and analytical replicates verify precision, as per ISO/IEC 17025:2017 and the 24th Edition of Standard Methods (ISO, 2017; Lipps et al., 2023). Certified reference materials, recovery tests, and calibration-verification standards were used to assess accuracy, metrological traceability, and calibration stability (Cantwell, 2025). Results below the applicable reporting limit were treated as censored observations. Variables dominated by censored results or showing zero variance were evaluated separately and excluded from multivariate analyses when appropriate. A complete major-ion charge-balance error could not be confirmed because validated bicarbonate and carbonate results were unavailable in the consolidated database. Therefore, the ±5% acceptance criterion reported in comparable groundwater studies was retained as a methodological reference rather than applied as a definitive validation result (Nefla et al., 2026). Results affected by analytical inconsistencies were reanalyzed, qualified, or excluded according to validated laboratory procedures.

2.7. Data processing and statistical analysis

Descriptive statistics were calculated for all groundwater variables. Before multivariate analysis, the dataset was screened for censored observations, analytical inconsistencies, outliers, and variables with zero variance. Outliers were retained unless field records or QA/QC procedures confirmed a measurement or transcription error. Ag, Al, As, Be, Cd, Ce, Co, Cr, Cu, Hg, Mo, Ni, P, Pb, Sb, Se, Sn, Ti, and Tl were excluded from PCA and HCA because their constant reported values prevented meaningful standardization. These variables were evaluated separately using their analytical qualifiers and applicable comparison values.

The remaining variables were converted to z-scores before being analyzed. The appropriateness of PCA was determined via the KMO test and Bartlett's sphericity test, with criteria of KMO of ≥0.60 and $p < 0.05$ being fulfilled to proceed further on. The applicability of the components was decided upon based on eigenvalue being greater than 1, the scree plot, explained variance, and hydrochemical implications. The Varimax with Kaiser normalization was used to facilitate interpretation (Omena et al., 2025). Euclidean distance and Ward's minimum variance linkage were used to perform HCA. Python with Google Colaboratory was used to do the statistical analyses and the figures, while QGIS Desktop 3.44.3 was used for spatial processing and preparing the final maps.

2.8. Spatial analysis and mapping

Validated hydrochemical data and well coordinates were integrated into QGIS Desktop 3.44.3, with complementary processing performed in Python. Coordinates were retained in UTM zone 17M, consistent with the original field database, and the resulting raster surfaces were clipped to the study area. Spatial patterns were estimated using inverse distance weighting (IDW) with a distance coefficient of p=2 (Figure 2).

Because IDW is sensitive to uneven sampling density and spatial clustering, the interpolated surfaces were treated as estimates rather than direct measurements at unsampled locations. Wells M2 and M3 shared the same horizontal coordinates but had different reported depths. Their parameter-specific arithmetic mean was therefore used only for two-dimensional interpolation, producing 24 unique spatial locations. The original M2 and M3 measurements remained independent in the descriptive and multivariate statistical analyses.

Interpolation performance was assessed through leave-one-out cross-validation using mean absolute error and root mean square error as performance indicators. Only validated variables showing measurable spatial variability were mapped. Variables with zero variance, repeated analytical-limit values, or unresolved analytical qualifiers were excluded from interpolation.

The resulting maps were interpreted as exploratory representations of groundwater-quality patterns and priority monitoring areas. They were not considered direct measurements between wells, confirmed contamination hotspots, contaminant-source maps, public-health risk maps, or formal assessments of aquifer vulnerability.

2.9. Groundwater Quality Index

Groundwater quality for potential drinking use was summarized using a weighted arithmetic Water Quality Index (WQI). This index provides an integrated screening measure but does not replace parameter-specific regulatory assessment or certify untreated groundwater as suitable for direct consumption.

Among the constituents of the WQI were pH, total dissolved solids (TDS), the amount of chloride,

sulfate, sodium, iron, manganese, and zinc, together with turbidity and hardness. Reference values were established through Peruvian legislation and the latest WHO directives (WHO, 2026; MINSA, 2010). Electrical conductivity has not been included in the assessment of mineralization, as TDS was calculated based on this parameter. Elements and indicators with a fixed value or value that were not clear were omitted.

Each parameter received an ordinal weight (ω_i) from 1 to 5 according to its health relevance, drinking-water acceptability, observed exceedances, and operational importance (Table 4). Relative weights were calculated as:

$$W_i = \frac{\omega_i}{\sum_{i=1}^{n} \omega_i}$$

where ω_i is the assigned ordinal weight, W_i is the normalized relative weight, and n is the number of parameters. The assigned weights summed to 33, and the normalized weights summed to 1.

For parameters other than pH, quality ratings were calculated as:

$$q_i = 100\left(\frac{C_i}{S_i}\right)$$

where Ci is the measured value and Si is the reference value. Because pH is defined by an acceptable range, its rating was calculated relative to the ideal value of 7.0:

$$q_pH = \begin{cases} 100\left(\frac{7.0 - C_i}{7.0 - 6.5}\right), & C_i < 7.0 \\ 100\left(\frac{C_i - 7.0}{8.5 - 7.0}\right), & C_i \geq 7.0 \end{cases}$$

The final index was obtained as:

$$WQI = \sum_{i=1}^{n} W_i q_i$$

WQI values were classified as excellent (≤25), good (>25 – 50), poor (>50 – 75), very poor (>75 – 100), or unsuitable (>100). The index was interpreted together with individual parameter exceedances.

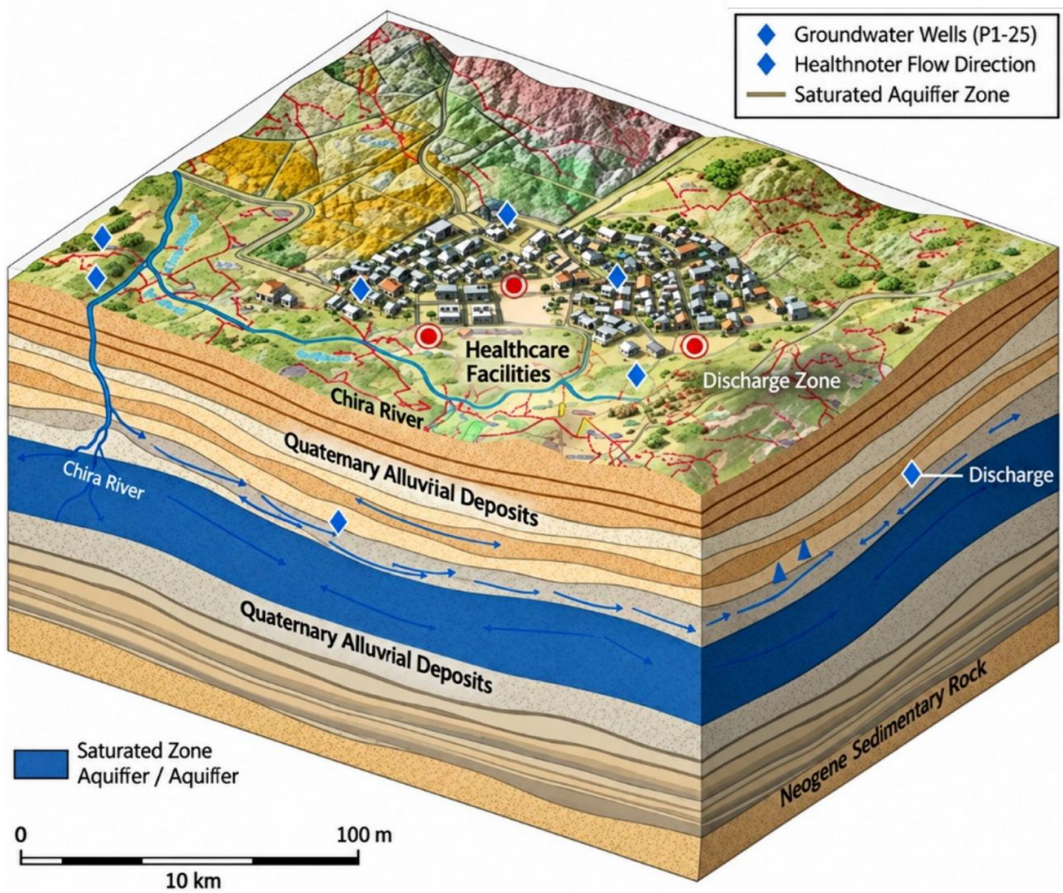


Figure 2. Integrated methodological workflow for hydrochemical, statistical, and spatial groundwater-quality assessment. Note: The workflow covers sampling, laboratory analysis, QA/QC, PCA, HCA, and IDW mapping. Python supported statistics, QGIS supported mapping, and invariant or censored variables were excluded from analyses.

Table 4
Parameters, reference values, and weights used in the WQI

Parameter	Unit	Reference value *Si*	Ideal value *Vi*	Weight *wi*	Relative weight *Wi*
pH	pH units	6.5 – 8.5	7.0	4	0.1212
Turbidity	NTU	5	0	3	0.0909
TDS	mg/L	1,000	0	4	0.1212
Total hardness	mg/L as $CaCO_3$	500	0	2	0.0606
Chloride	mg/L	250	0	4	0.1212
Sulfate	mg/L	250	0	4	0.1212
Sodium	mg/L	200	0	4	0.1212
Iron	mg/L	0.30	0	2	0.0606
Manganese	mg/L	0.40	0	5	0.1515
Zinc	mg/L	3.0	0	1	0.0303
Total				33	1.0000

Note. *Si* is the reference value, *Vi* the ideal value, *wi* the assigned weight, and *Wi* the normalized weight. Weights were study-specific, not statutory. EC, invariant variables, and analytically unresolved parameters were excluded from WQI.

3. Results and discussion

3.1. Physicochemical characteristics of groundwater

Groundwater characteristics varied considerably among the 25 wells (Table 5). Water temperature ranged from 26.3 to 31.7 °C, while pH ranged from 6.90 to 8.24, remaining within the comparison range of 6.5 – 8.5. Turbidity ranged from 0.18 to 5.40 NTU, with two wells (8%) exceeding 5 NTU. Electrical conductivity ranged from 656 to 17,290 µS/cm and averaged 3,360.92 µS/cm, whereas TDS ranged from 347 to 5,440 mg/L and averaged 1,368.72 mg/L. Overall, 44% of wells exceeded 1,500 µS/cm for EC, and 40% exceeded 1,000 mg/L for TDS. Chloride ranged from 80.97 to 4,522.60 mg/L and exceeded 250 mg/L in 88% of wells. Sulfate ranged from 55.93 to 1,648.67 mg/L and exceeded 250 mg/L in 56% of wells. Together, EC, TDS, chloride, and sulfate showed substantial variation in groundwater mineralization across the monitoring network. These comparisons should be interpreted according to their intended use because WHO drinking-water guidance differs from the category-specific environmental criteria established for receiving water bodies (WHO, 2026; MINAM, 2017). The spatial distribution of TDS, electrical conductivity, pH, and turbidity across the sampled groundwater wells is shown in Figure 3.

Groundwater chemistry in Sullana was heterogeneous: EC ranged from 656 to 17,290 µS/cm, TDS from 347 to 5,440 mg/L, chloride from 80.97 to 4,522.60 mg/L, and sulfate from 55.93 to 1,648.67 mg/L. These findings indicate that mineralization was the main source of chemical variation among the sampled wells. The groundwater found in semi-arid aquifers generally mirrors the results of evaporation, mineral dissolution, weathering, cation exchange, return irrigation flow, and saline-water mixing (Mukherjee & Singh, 2022; Salman et al., 2024; Wang et al., 2026; Ximenes et al., 2026). Irrigation might recharge the aquifers while degrading the water quality. Water percolating through the soil can move the salt, fertilizers, and pesticides that have been deposited in the soil, while water used for irrigation losses its quality upon evaporation. Similar effects were also noticed in semi-arid aquifers (Alexakis, 2022; Missaoui et al., 2026; Wang et al., 2026; Sanad et al., 2025) but cannot be quantified in relation to Sullana without seasonal monitoring of the irrigation system, drainage, soil, and groundwater.

Urban sources may include sewer leakage, septic systems, untreated wastewater, solid-waste leachate, and urban runoff. Studies have used NO_3^-, NH_4^+, phosphate, microbial indicators, landuse information, and temporal monitoring to identify these pressures (Alsabti et al., 2023; Mêlo et al., 2023; Mester et al., 2026). Because these indicators were unavailable in Sullana, wastewater and fertilizer input remain plausible rather than demonstrated.

3.2. Major ion hydrochemistry

The concentration of major ions differed significantly in the analyzed wells. The concentration of calcium ion in water samples varied between 44.80 - 404.28 mg/L, magnesium between 4.62 - 72.21 mg/L, sodium between 26.51 - 2,575.58 mg/L, and potassium between 0.31 - 8.01 mg/L. The level of sodium ion in the wells exhibited obvious differences, thus indicating considerable variation in groundwater mineralization. The concentration of chloride ions ranged from 80.97 to 4,522.60 mg/L with a mean value of 858.23 mg/L. The concentration of sulfate ion ranged from 55.93 to 1,648.67 mg/L with an average value of 386.39 mg/L. Chloride ion concentration exceeds 250 mg/L in 88% of wells and sulfate in 56%, which is in line with the exchangeable cation results.

Table 5
Descriptive statistics of groundwater physicochemical parameters (n = 25)

Parameter	Unit	Mean	SD	Min	Max	Comparison value	Wells above value
Temperature	°C	29.12	1.56	26.30	31.70	Not established	Not applicable
pH	pH units	7.40	0.29	6.90	8.24	6.5 – 8.5	0%
Turbidity	NTU	1.99	1.36	0.18	5.40	5.0	8%
EC	µS/cm	3,360.92	3,808.41	656	17,290	1,500	44%
TDS	mg/L	1,368.72	1,270.07	347	5,440	1,000	40%
Chloride	mg/L	858.23	948.03	80.97	4,522.60	250	88%
Sulfate	mg/L	386.39	407.40	55.93	1,648.67	250	56%

Note: SD = standard deviation; EC = electrical conductivity; TDS = total dissolved solids. Statistics use 25 samples. ECA criteria are category-specific, not drinking-water standards (MINAM, 2017).

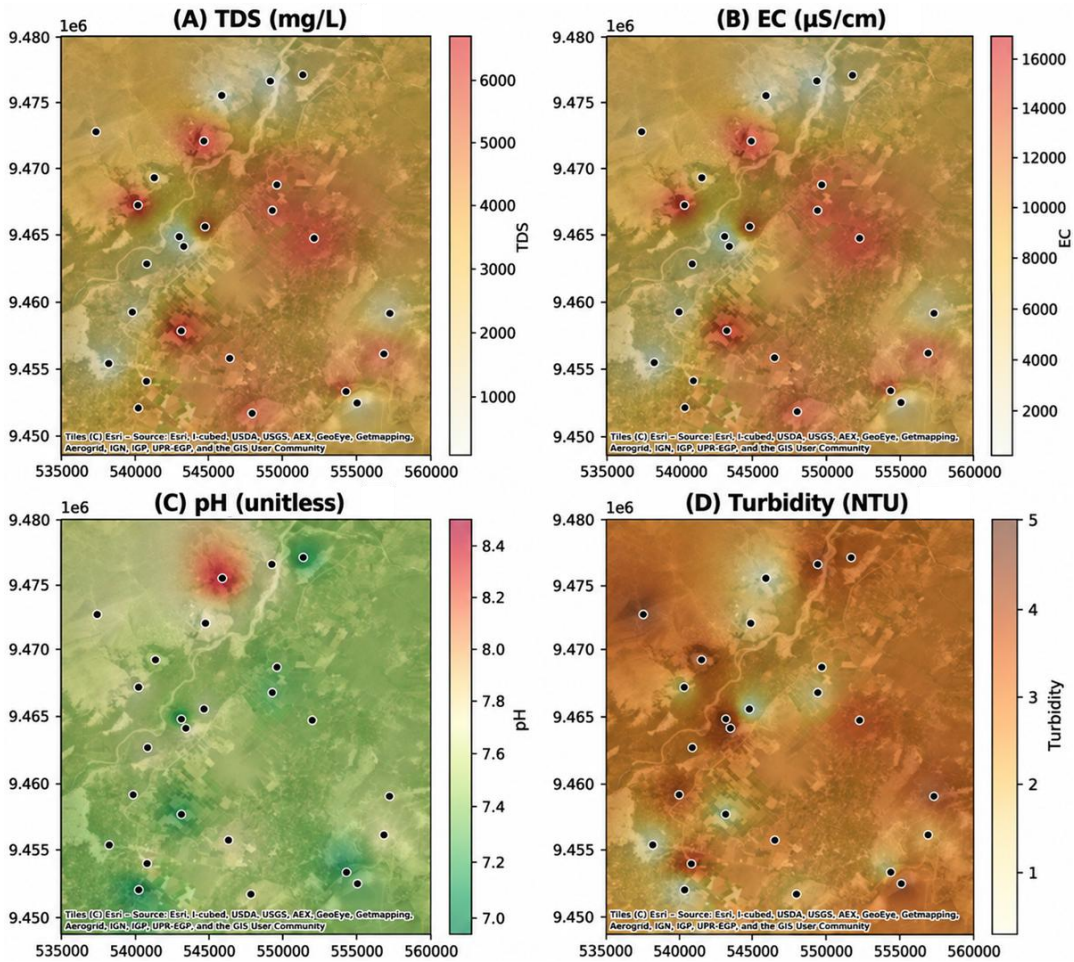


Figure 3. Spatial distribution of selected groundwater physicochemical parameters in the sampled study domain: (A) total dissolved solids, (B) electrical conductivity, (C) pH, and (D) turbidity. Note: IDW used 24 unique locations with p = 2. M2–M3 parameter means supported interpolation only. Black symbols mark sampled wells; color gradients represent spatial estimates, not measurements or confirmed contamination zones.

Piper facies could not be completed since validated bicarbonate information was not available. Major ion patterns have been interpreted to represent composition differences rather than direct evidence of the recharge, discharge, or directions of groundwater flow. The simultaneous increase in Na^+, Cl^-, and SO_4^{2-} can be explained by evaporation, water–rock interaction, salinization of evaporites, irrigation return flow, cation exchange, etc. Indeed, similar signatures can be obtained through various processes, hence, Na–Cl dominance and high EC do not serve as evidence of seawater intrusion (Wurl et al., 2023).

PCA supported this finding by stating that PC1 was able to explain the 56.07% of the overall variance, placing EC, TDS, Na^+, Cl^-, SO_4^{2-}, Ca^{2+}, Mg^{2+} ions on a wide mineralization continuum. Such behavior was reported in various coastal and irrigation

aquifers (Slama et al., 2022; Ji et al., 2024; Dhakate, 2024; Sanad et al., 2025; Ha et al., 2026). However, PCA identifies covariance rather than causality. Therefore, PC1 cannot be attributed exclusively to seawater intrusion, evaporite dissolution, or irrigation return flow.

The analysis included separate evaluations of Na^+/Cl^-, Cl^-/SO_4^{2-}, Ca^{2+}/Na^+, and the cation Gibbons ratio in addition to the other parameters. The influence of Br^- and stable isotopes proved elusive. Consequently, oceanic influence was treated as hypothesis rather than a confirmed source. Reliable discrimination necessitates ionic ratios, modeling mineral saturation data and/or Br^-/Cl^- or Cl^-/Br^- ratios together with stable isotopes and also representative end members (El Mountassir & Bahir, 2023).

3.3. Ionic ratios and Gibbs diagrams

The processes involved in the mineralization of groundwater were examined using molar composition ratios. The value of Na^+/Cl^- was found to be between 0.09 and 1.82 with a mean of 0.44. In the case of the nineteen wells, the Na^+/Cl^- values were recorded at below 0.80, while three wells were in the Na^+/Cl^- range of 0.80 - 1.20, and another three wells had Na^+/Cl^- values above 1.20. Furthermore, the values near 1.00 can either indicate dissolution of halite or mixing of saline waters, but in case of not being equal to 1.00, the reason can be determined by ion exchange, mineral weathering, return flow from irrigation or selective ion removal.

The Cl^-/SO_4^{2-} ratio between the different wells varies from a minimum of 1.15 to a maximum of 21.71 with a ratio above one in every well hence indicative of the prevalence of chloride without a clear source determination. Marine mixing occurs distinctly from evaporite dissolution that will require several ion ratios and geochemical indicators (Wurl et al., 2023).

The ratio of Ca^{2+}/Na^+ varied from 0.04 to 1.09 and fell below one in 23 wells, indicating a predominance of sodium. The cationic Gibbs Ratio $Na^+/(Na^+ + Ca^{2+})$ varied between 0.48 and 0.96 and demonstrated positive correlation with TDS (Spearman's $\rho = 0.739$, $p < 0.001$). Therefore, the groundwater with the highest mineral content in general is characterized by a greater predominance of sodium.

Because data related to bicarbonates were unavailable, it was not possible to measure the anionic Gibbs ratio Cl-/(Cl- + HCO_3^-). The absence of Br^- and $\delta^{18}O$ and δ^2H made it impossible to determine the contribution of processes like evaporation, evaporitic dissolution, irrigation return flow, inheritance salinity, and seawater mixing (El Mountassir & Bahir, 2023). The summary statistics of the molar ionic ratios, including their minimum, median, maximum, and main interpretative results, are presented in Table 6. Ionic ratios provided additional insight into mineralization, although none can independently identify a salinity source. Na^+/Cl^- ranged from 0.09 to 1.82, with 19 wells below 0.80. While values close to 1 may indicate either halite dissolution or mixing of saline waters, values more distant from the unity may be attributed to ion exchanges, weathering of rock, irrigation return water or selective ion extraction (Slama et al., 2022; Gomes et al., 2023; Dhakate, 2024; Ha et al., 2026).

The Cl^-/SO_4^{2-} range of 1.15-21.71 indicates the dominance of chloride but does not signify its source. The observed range can be produced by marine mixing, halite dissolution, irrigation-water reuse, wastewater intrusion, or inherited salinity. Identification of the exact source needs more reliable evidence, such as Br^-, Cl^-/Br^-, sulfate isotopes, mineral saturation indices, and representative values (Zhang et al., 2023; Jiang et al., 2023).

In 23 of the wells, the Ca^{2+}/Na^+ ratio was less than one. Additionally, the relation of Gibbs with TDS was strong, with a correlation coefficient of 0.739 ($p < 0.001$), which showed the increasing dominance of Na+ in the more mineralized aquifers. Nonetheless, it has been noted that Gibbs plots are screening tools and not indicators of the specific processes involved (Mukherjee & Singh, 2022; Zeng et al., 2024; Manu et al., 2026).

The anionic Gibbs ratio was not calculated because validated HCO_3^- data were unavailable. This limitation also prevented Revelle–Simpson, RSC, complete CAI, HFE-D, and Durov analyses. Future campaigns should include HCO_3^-, CO_3^{2-}, Br^-, $\delta^{18}O$, δ^2H, and sulfate isotopes to distinguish evaporation, mineral dissolution, irrigation recycling, seawater intrusion, and palaeosalinity (El Mountassir & Bahir, 2023; Ji et al., 2024; Azari & Tabari, 2024).

Table 6
Summary of molar ionic ratios

Indicator	Minimum	Median	Maximum	Main result
Na^+/Cl^-	0.09	0.44	1.82	19 of 25 wells below 0.80
Cl^-/SO_4^{2-}	1.15	5.70	21.71	All wells above 1
Ca^{2+}/Na^+	0.04	0.44	1.09	23 of 25 wells below 1
$Na^+/(Na^+ + Ca^{2+})$	0.48	0.69	0.96	Increased significantly with TDS

Note. The ionic ratios are computed from the concentrations which are converted in mmol L^{-1}. The supplied values are interpretative indicators instead of diagnostic criteria. To properly find the source of salinity in the groundwater, it is necessary to use many different ratios and independent tracers.

3.4. Trace metal distribution

The patterns for different trace elements were dissimilar for quantitated and unquantitated variables. While iron, manganese, and zinc concentrations varied across diverse wells, the concentrations of arsenic, lead, cadmium, copper, and some other elements were the same for all 25 samples. Thus, those values were considered as possible substitutes for analytical limits and were preliminary pending checks against the limits of detection (LOD), limits of quantifications (LOQ), reporting limits, and qualifiers created for the lab analysis. Hence, the exclusion of these values from PCA and HCA was accounted due to the lack of any variance, not because they were absent from groundwater.

The concentration of iron was between 0.004 and 0.156 mg/L, and the mean concentration was 0.034 ± 0.047 mg/L. Anthropogenic sources of manganese varied from 0.0002 to 2.2974 mg/L, while the mean was 0.177 ± 0.503 mg/L. There were three wells, or 12% of the total, that had manganese concentrations greater than 0.40 mg/L. Measurements of zinc ranged from 0.0004 to 0.240 mg/L with all samples exceeding 3.0 mg/L (Table 7).

The comparisons made with relation to regulations have been done following the WHO guidelines alongside the Law on Drinking Water in Peru, rather than using environmental standards (WHO, 2026; MINSA, 2010). The datasets used do not show information about local geochemical background. Reliable source attribution means measuring the redox status, proving the mineralogical composition, having representative observation wells, and knowing the characteristics of the region in terms of background.

The analysis with respect to trace elements requires separating the recorded concentrations from the non-detect readings, as well as zero readings. It is found that Fe, Mn, and Zn levels show variability across the wells, while As, Pb, Cd, and Cu concentrations provide uniformity over the sampling points. In particular, the reported levels of As (0.008 mg/L), Pb (0.006 mg/L), Cd (0.0004 mg/L), and Cu (0.001 mg/L) can hardly be interpreted as similar concentrations in the environment. At least, it would be reasonable to assume that the provided data may represent alternative readings at levels lower than the maximum detection threshold or rounded in a wrong manner. Research points out the significance of the following items in environmental assessments: calibration, empty or blank readings, repeatability, reference materials, recovery rates, precision, detection thresholds, and quantification thresholds (Zhou et al., 2023; Benaafi et al., 2023; Sugumaran et al., 2026; Nefla et al., 2026). It is recommended not to use censored variables in the analysis (Tziritis et al., 2024).

The concentration of Fe was between 0.004 mg/L and 0.156 mg/L and was lower than 0.30 mg/L. However, for Mn, the value ranged from 0.0002 to 2.2974 mg/L. The values of M12, M15, and M17 exceeded 0.40 mg/L (Figure 4). Studies have reported levels of Mn in the Seridó aquifer in Brazil similar to those measured in M12, M15, and M17, but this does not mean that they have a common origin since the two aquifers differ in hydrogeology and lithology (Araújo et al., 2026).

There was a distinction between the Fe–Mn association in PC2 and the dominant-ion mineralization but it did not sufficiently indicate reductive dissolution. To provide confirmation, one must have secured DO and ORP data, Fe(II) and Fe(total) values, filtered/unfiltered fractions, alkalinity, ammonium, and sulfide levels, as well as sediment mineral composition (Liang et al., 2022; Zhi et al., 2022). To create a geochemical background for a local area, it is important to have sufficient representative reference wells, lithological data, hydrochemical data, and enough observations from uncensored data (Voutchkova et al., 2021). Hence, Mn is a question that has been localized, whereas As, Pb, Cd, and Cu must be subjected to laboratory analysis before regulatory and health-related conclusions are drawn.

Table 7
Trace elements and comparison with drinking-water criteria (n = 25)

Element	Unit	Result	Minimum–maximum	Comparison value	Wells above value, n (%)
Arsenic	mg/L	0.008 in all samples*	Not applicable	0.010	Not determined*
Lead	mg/L	0.006 in all samples*	Not applicable	0.010	Not determined*
Cadmium	mg/L	0.0004 in all samples*	Not applicable	0.003	Not determined*
Copper	mg/L	0.001 in all samples*	Not applicable	2.000	Not determined*
Iron	mg/L	0.034 ± 0.047	0.004–0.156	0.300	0 (0%)
Manganese	mg/L	0.177 ± 0.503	0.0002–2.2974	0.400	3 (12%)
Zinc	mg/L	0.033 ± 0.046	0.0004–0.240	3.000	0 (0%)

Note: Mean ± standard deviation is used to report results where applicable, and the same As, Pb, Cd, and Cu figures need to be checked against LOD, LOQ, limits of reporting, and the qualifiers prior to computing detection rates and compliance rates (WHO, 2026; MINSA, 2010).

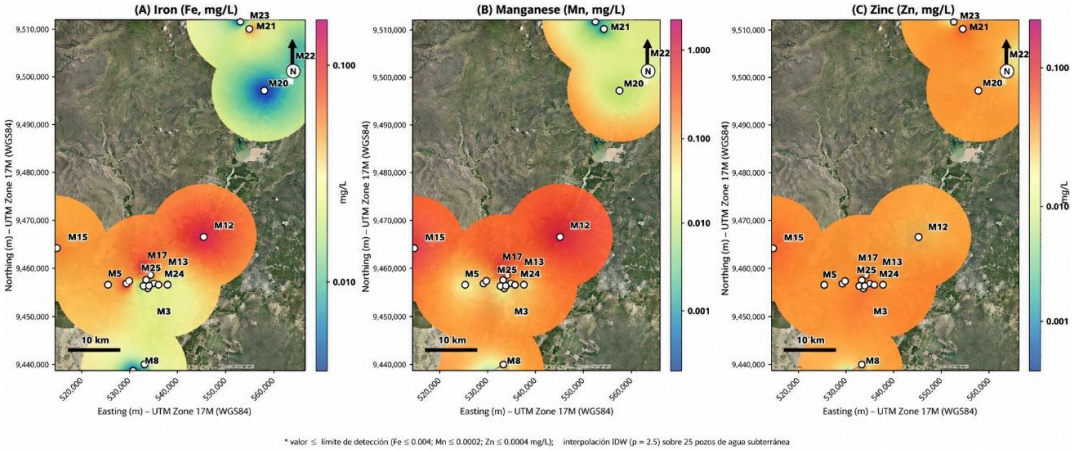


Figure 4. Spatial distribution of quantified trace elements in groundwater: (A) iron, (B) manganese, and (C) zinc Note: IDW mapped validated, variable elements using 24 locations and p = 2. M2–M3 means represented their shared coordinate. Colors show estimates, not sources; invariant As, Pb, Cd, and Cu were excluded.

3.5. Multivariate statistical analysis

3.5.1. Principal Component Analysis (PCA)

PCA of standardized concentrations of EC, TDS, Na^+, Cl^-, SO_4^{2-}, Ca^{2+}, Mg^{2+}, Fe, and Mn was conducted. The sampling adequacy was verified with KMO value of 0.685 and having passed the Bartlett's test ($\chi 2(36) = 240.85$, $p < 0.001$) the dataset was acknowledged to be good for extraction of the components (Omena et al., 2025). Two components with eigenvalues above 1 accounted for 78.46% of total variance. After the Varimax rotation, it was determined that 56.07% was accounted for by principal component PC1, with strong positive loadings for EC, Na^+, Cl^-, SO_4^{2-}, Ca^{2+}, and Mg^{2+}, while TDS demonstrated a less significant load (Table 8). The interpretation of PC1 suggests that it reflects the overall mineralization by the major ions instead of a purely Na–Cl process. The second principal component (PC2) explained 22.38% of the total variance, and is represented mainly by Fe and Mn, which were used to differentiate their signal from that of the major ions. Nonetheless, a redox analysis is still possible, given that there were no ORP data and the DO measurements need to be confirmed. The well locations and variables within the two elements used are displayed in Figure 5a. No constant variables were considered, since PCA is concerned only with covariance patterns and not with the sources of contaminants or the hydrogeochemical processes involved (Ximenes et al., 2026).

PCA supported this finding by stating that PC1 was able to explain the 56.07% of the overall variance, placing EC, TDS, Na^+, Cl^-, SO_4^{2-}, Ca^{2+}, Mg^{2+} ions on a wide mineralization continuum. Such behavior was reported in various coastal and irrigation aquifers (Slama et al., 2022; Ji et al., 2024; Dhakate, 2024; Sanad et al., 2025; Ha et al., 2026). However, PCA identifies covariance rather than causality. Therefore, PC1 cannot be attributed exclusively to seawater intrusion, evaporite dissolution, or irrigation return flow.

Table 8
Rotated PCA loading matrix

Variable	PC1: Mineralization	PC2: Fe–Mn variability
EC	**0.953**	−0.141
TDS	0.514	−0.271
Na^+	**0.958**	−0.151
Cl^-	**0.955**	−0.072
SO_4^{2-}	**0.809**	−0.062
Ca^{2+}	**0.871**	0.280
Mg^{2+}	**0.791**	0.511
Fe	−0.015	**0.848**
Mn	−0.077	**0.911**
Variance explained (%)	**56.07**	**22.38**
Cumulative variance (%)	**56.07**	**78.46**

Note. PCA used z-score standardization and Varimax rotation. Loadings ≥0.70 were bolded. KMO = 0.685; Bartlett's test was statistically significant.

3.5.2. Hierarchical Cluster Analysis (HCA)

Hierarchical cluster analysis used the same nine z-score-standardized variables as PCA: EC, TDS, Na^+, Cl^-, SO_4^{2-}, Ca^{2+}, Mg^{2+}, Fe, and Mn. Euclidean distance and Ward's minimum-variance linkage separated the 25 wells into three chemical groups (Figure 5b). Cluster 1 contained 20 wells and showed the lowest overall mineralization, with mean EC and TDS values of 1,951.65 µS/cm and 930.30 mg/L, respectively. Cluster 2 included M1, M7, M8, and M9 and showed higher mineralization, with mean EC and TDS values of 6,925.00 µS/cm and 3,674.00 mg/L. Mean Na^+, Cl^-, and SO_4^{2-} concentrations were 869.91, 1,590.76, and 747.61 mg/L, respectively.

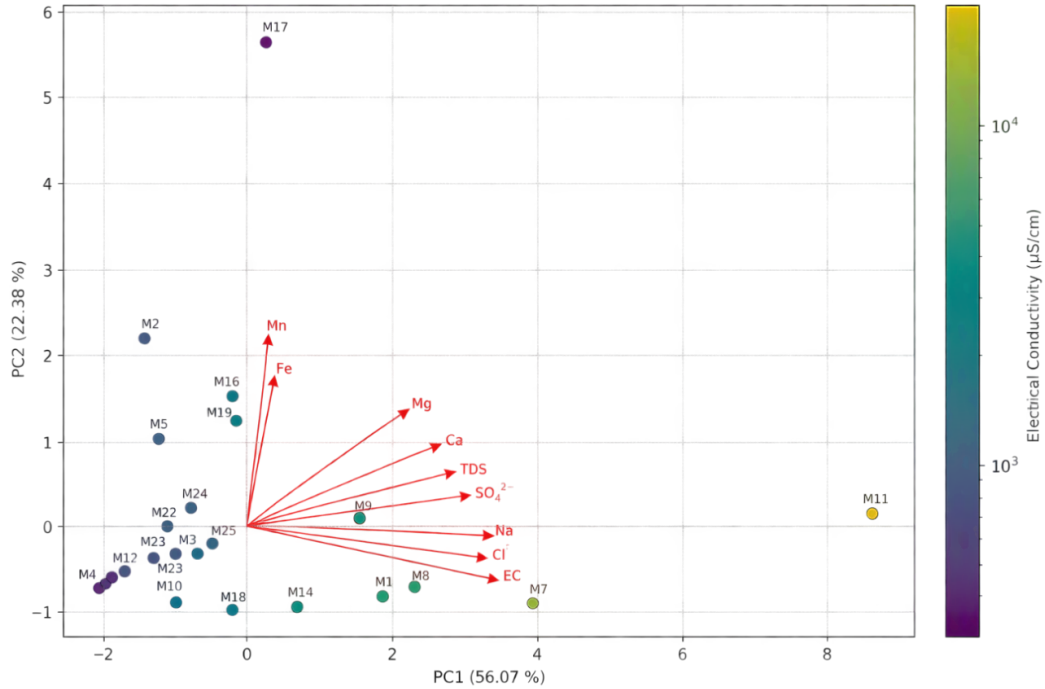


Figure 5a. PCA biplot of groundwater physicochemical and chemical variables. Note: The biplot projects 25 wells and nine variables. PC1 represents mineralization (56.07%); PC2 reflects Fe–Mn variability (22.38%). Together, both explain 78.46%; vector direction and length indicate association and contribution.

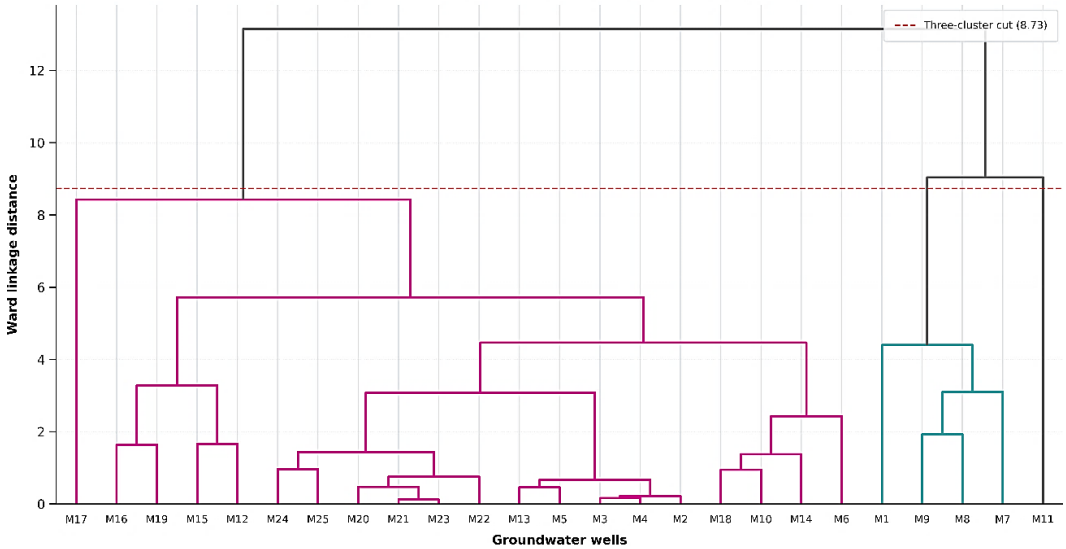


Figure 5b. Dendrogram of the hierarchical cluster analysis of groundwater wells. Note. The dendrogram used nine standardized variables, Euclidean distance, and Ward linkage. Cutting at 8.73 yielded three clusters of 20, four, and one well, representing chemical similarity, not hydrogeological zones.

Cluster 3 contained only M11, which had the highest EC, Na^+, Cl^-, SO_4^{2-}, Ca^{2+}, and Mg^{2+} values but an unexpectedly low TDS relative to EC. Because TDS was instrument-derived, this record requires verification (Table 9). M11 was therefore treated as a hydrochemical outlier rather than a spatially extensive groundwater regime.

Exploratory ANOVA showed differences among clusters for EC, TDS, Na^+, Cl^-, SO_4^{2-}, Ca^{2+}, and Mg^{2+} ($p < 0.001$), with the largest F-values for Na^+ ($F = 75.19$), Cl^- ($F = 51.08$), and EC ($F = 49.26$). Differences in pH, Fe, and Mn were not significant. Cluster membership indicates chemical similarity rather than direct evidence of recharge, discharge, contamination sources, contemporary seawater intrusion, or aquifer vulnerability.

The HCA drilled 20 holes in Cluster 1, grouped M1, M7, M8 and M9 in Cluster 2, and recognized M11 as

a hydrochemical outlier, similar to the finding of Hamma et al. (2025). Chemical clusters do not define groundwater movement routes. It is necessary to use screened intervals, piezometric measurements, hydraulic gradients, and foreign tracers in order to carry out hydrogeological interpretation (Hou et al., 2024; Narvaez-Montoya et al., 2024; Ximenes et al., 2026).

3.5.3. Integrated multivariate patterns

PCA and HCA provided complementary evidence of groundwater-chemistry variability. PCA showed that major-ion composition contributed strongly to PC1, while HCA differentiated wells mainly according to EC, TDS, Na^+, Cl^-, SO_4^{2-}, Ca^{2+}, and Mg^{2+} concentrations. The four wells grouped in Cluster 2 showed comparatively high salinity-related values, whereas M11 formed a separate cluster because of its distinct chemical composition. The spatial maps illustrated the distribution of EC, TDS, chloride, and sulfate across the monitoring network. However, the relationship between cluster membership and mapped patterns was interpreted descriptively and was not considered evidence of groundwater-flow direction or salinity sources. Distinguishing among evaporation, evaporite dissolution, irrigation return flow, inherited salinity, and marine mixing requires the ionic ratios discussed in Section 3.3 and, ideally, independent tracers such as Br^-, Cl^-/Br^-, $\delta^{18}O$, and δ^2H.

3.5.4. Heatmap visualization

The standardized heatmap supported the multivariate findings by showing the relative variation in EC, TDS, Na^+, Cl^-, SO_4^{2-}, Ca^{2+}, Mg^{2+}, Fe, and Mn across the 25 wells (Figure 5c). Warm colors indicate standardized values above the mean of each variable, whereas cool colors indicate values below the mean.

EC, TDS, Na^+, Cl^-, SO_4^{2-}, Ca^{2+}, and Mg^{2+} showed broadly similar patterns, consistent with their positive PC1 loadings and contribution to HCA separation. Fe and Mn were associated with PC2 and displayed spatially different distributions. Therefore, the heatmap illustrates statistical covariation but does not demonstrate that associated parameters share a single geochemical or anthropogenic source.

Constant-value variables, including As, Pb, Cd, and Cu, were excluded because zero variance prevents meaningful z-score standardization. In addition, their repeated database values may represent analytical-limit substitutions rather than genuine spatial variation.

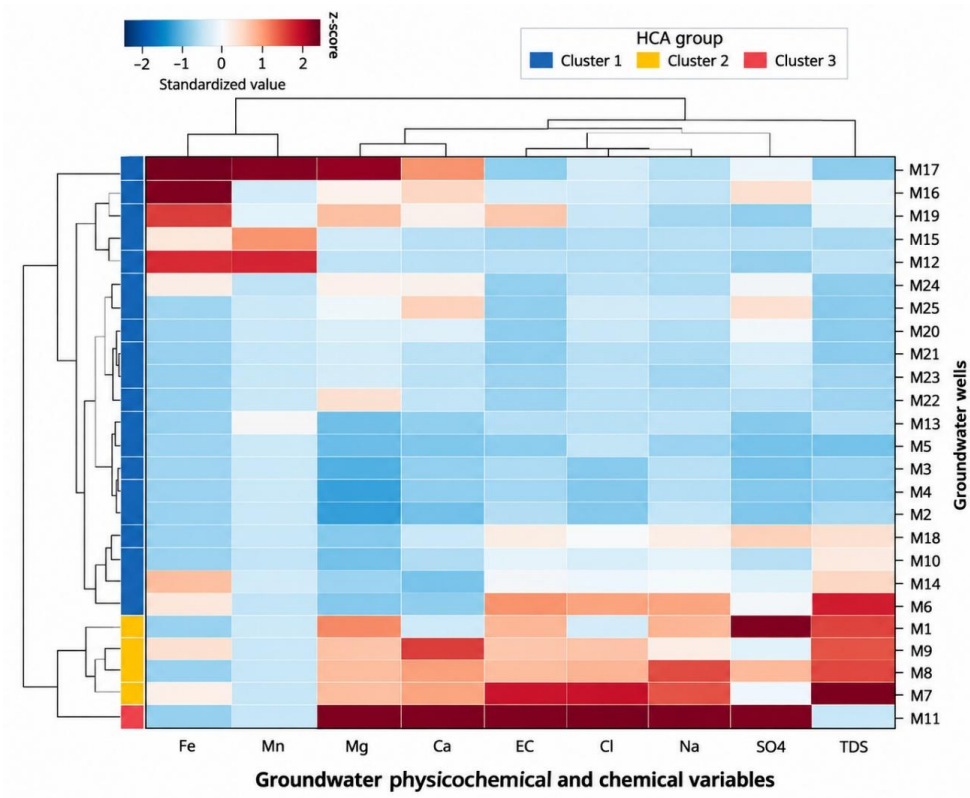


Figure 5c. Heatmap of standardized groundwater physicochemical and chemical variables. Note. Colors show standardized values: warm above-average and cool below-average. Ward clustering orders wells and variables. The side bar identifies three clusters; invariant or censored variables were excluded from analysis.

Table 9
Mean hydrochemical values by HCA cluster

Parameter	Unit	Cluster 1 (n = 20)	Cluster 2 (n = 4)	Cluster 3 (n = 1)	F-value	p-value
EC	µS/cm	1,951.65	6,925.00	17,290.00	49.26	<0.001
TDS	mg/L	930.30	3,674.00	916.00	20.76	<0.001
Na^+	mg/L	167.96	869.91	2,575.58	75.19	<0.001
Cl^-	mg/L	528.51	1,590.76	4,522.60	51.08	<0.001
SO_4^{2-}	mg/L	251.04	747.61	1,648.67	18.18	<0.001
Ca^{2+}	mg/L	85.62	172.11	404.28	28.94	<0.001
Mg^{2+}	mg/L	18.24	35.18	72.21	11.77	<0.001
pH	pH units	7.44	7.19	7.44	1.41	0.265
Fe	mg/L	0.038	0.024	0.004	0.34	0.714
Mn	mg/L	0.220	0.005	0.0002	0.35	0.708

Note. Clusters were obtained from z-score-standardized EC, TDS, Na^+, Cl^-, SO_4^{2-}, Ca^{2+}, Mg^{2+}, Fe, and Mn using Euclidean distance and Ward's minimum-variance linkage. Cluster numbers were ordered according to increasing mean EC. ANOVA results involving Cluster 3 are exploratory because it contains only M11.

3.6. Regulatory compliance

Groundwater results were assessed against the values established in the Peruvian Regulation on Water Quality for Human Consumption and current World Health Organization guidance (MINSA, 2010; WHO, 2026). This comparison evaluated the quality of untreated groundwater but did not certify its suitability for direct consumption. Peru's Environmental Quality Standards were not used as the principal benchmark because they classify receiving water bodies according to category and intended use.

Eleven wells (44%) exceeded 1,500 µS/cm for electrical conductivity, while 10 wells (40%) exceeded 1,000 mg/L for total dissolved solids. Chloride exceeded 250 mg/L in 22 wells (88%), and sulfate exceeded 250 mg/L in 14 wells (56%). Overall, 22 wells exceeded at least one mineralization-related comparison value. All Cluster 2 wells exceeded the comparison values for electrical conductivity, total dissolved solids, chloride, and sulfate. M11 exceeded the values for electrical conductivity, chloride, and sulfate, while Cluster 1 also included several wells with exceedances.

Iron and zinc remained below 0.30 and 3.0 mg/L, respectively, whereas manganese exceeded 0.40 mg/L in three wells (12%). The repeated As, Pb, Cd, and Cu results require verification against the laboratory limit of detection (LOD), limit of quantification (LOQ), reporting limit, and analytical qualifiers. Values below the LOD indicate that the analyte was not detected under the applied method. Values between the LOD and LOQ may indicate detection, but they cannot be quantified reliably (Table 10).

3.7. Groundwater Quality Index (WQI)

The Weighted Arithmetic Water Quality Index showed a wide variation in the monitoring network (Table 11). It consisted of pH, turbidity, TDS, total hardness, chloride, sulfate, sodium, iron, manganese, and zinc, using the weights and classifications described in Section 2.9. The reference values were based on the Peruvian drinking-water regulation and the current recommendations of WHO (MINSA, 2010; WHO, 2026).

WQI values ranged from 27.23 at M4 to 495.92 at M11, with a median of 87.77. No well was classified as excellent. Four wells (16%) were classified as good, seven (28%) as poor, five (20%) as very poor, and nine (36%) as unsuitable. Therefore, 84% of the wells were classified as poor, very poor, or unsuitable under the adopted methodology. The good-quality category included M2, M3, M4, and M5, while the highest WQI values were recorded at M11, M7, M8, M1, M6, M17, and M9.

Chloride, TDS, sodium, and sulfate were the main contributors at the most affected wells. Manganese also contributed substantially to M12, M15, and M17, where concentrations exceeded 0.40 mg/L. These findings broadly agreed with the HCA results: all Cluster 2 wells and M11 in Cluster 3 were unsuitable, whereas Cluster 1 ranged from good to unsuitable.

As, Pb, Cd, Cu, and other invariant elements were excluded because their repeated values may represent analytical-limit substitutions rather than quantified concentrations. Accordingly, the WQI was interpreted as a screening summary, not as evidence that untreated groundwater was safe for consumption. A favorable category could not override an individual exceedance, an unresolved analytical qualifier, or the absence of microbiological assessment. The WQI for M11 remains provisional because its recorded TDS was unexpectedly low relative to EC.

WQI values ranged from 27.23 at M4 to 495.92 at M11, with a median of 87.77. Four wells were classified as good, seven as poor, five as very poor, and nine as unsuitable. Therefore, 84% of wells were classified as poor, very poor, or unsuitable under the adopted formulation. WQI classifications depend on the selected parameters, weights, reference values, and category boundaries (Alexakis, 2022; Awasthi et al., 2023; Dougha et al., 2026;

Ximenes et al., 2026). The index should therefore be interpreted together with individual concentration and parameter-specific exceedances. EC was excluded from the WQI because TDS was derived from conductivity, thereby avoiding duplicate representation of mineralization. This differs from indices that include both EC and TDS and may consequently give greater weight to salinity (El Mountassir & Bahir, 2023; Sanad et al., 2025). Irrigation indicators revealed additional constraints. SAR ranged from 0.91 to 31.00, with 18 wells below 10, while Na% ranged from 26.87% to 90.97%, with six wells above 80%. Eleven wells had EC values above 2,250 µS/cm, confirming that a low SAR does not eliminate salinity risk (Pitchaimani et al., 2026). RSC could not be calculated because validated HCO_3^- and CO_3^{2-} data were unavailable. Irrigation recommendations should also consider soil texture, drainage, crop tolerance, leaching requirements, and irrigation methods.

Table 10
Regulatory comparison of groundwater-quality parameters

Parameter	Comparison value	Maximum recorded value	Wells exceeding, n	Wells exceeding, %
pH	6.5–8.5	8.24	0	0
Turbidity	5 NTU	5.40 NTU	2	8
EC	1,500 µS/cm	17,290 µS/cm	11	44
TDS	1,000 mg/L	5,440 mg/L	10	40
Chloride	250 mg/L	4,522.60 mg/L	22	88
Sulfate	250 mg/L	1,648.67 mg/L	14	56
Iron	0.30 mg/L	0.156 mg/L	0	0
Manganese	0.40 mg/L	2.2974 mg/L	3	12
Zinc	3.0 mg/L	0.240 mg/L	0	0
Arsenic	0.010 mg/L	Analytical qualifier pending	Not determined*	Not determined*
Lead	0.010 mg/L	Analytical qualifier pending	Not determined*	Not determined*
Cadmium	0.003 mg/L	Analytical qualifier pending	Not determined*	Not determined*
Copper	2.0 mg/L	Analytical qualifier pending	Not determined*	Not determined*

Note. Comparison values follow Peru's drinking-water regulation and WHO guidance (MINSA, 2010; WHO, 2026). Identical As, Pb, Cd, and Cu values require laboratory confirmation before reporting non-detection or regulatory compliance.

Table 11
Groundwater Quality Index and classification of the monitored wells

Well	WQI	Quality category	Main contributing parameters	HCA cluster
M1	202.07	Unsuitable	Sulfate, Na, TDS	2
M2	29.72	Good	TDS, Na, chloride	1
M3	29.73	Good	TDS, turbidity, chloride	1
M4	27.23	Good	TDS, pH, Na	1
M5	38.59	Good	Chloride, TDS, turbidity	1
M6	198.22	Unsuitable	Chloride, Na, TDS	1
M7	297.70	Unsuitable	Chloride, Na, TDS	2
M8	236.40	Unsuitable	Chloride, Na, TDS	2
M9	170.73	Unsuitable	Chloride, TDS, Na	2
M10	88.03	Very poor	Chloride, TDS, Na	1
M11	495.92[1]	Unsuitable	Chloride, Na, sulfate	3
M12	95.20	Very poor	Mn, chloride, TDS	1
M13	52.83	Poor	Chloride, TDS, Na	1
M14	116.76	Unsuitable	Chloride, Na, TDS	1
M15	87.77	Very poor	Mn, chloride, sulfate	1
M16	97.04	Very poor	Chloride, sulfate, TDS	1
M17	170.92	Unsuitable	Mn, chloride, sulfate	1
M18	122.76	Unsuitable	Chloride, Na, sulfate	1
M19	69.41	Poor	Chloride, TDS, hardness	1
M20	66.27	Poor	Chloride, sulfate, TDS	1
M21	53.83	Poor	Chloride, sulfate, TDS	1
M22	51.46	Poor	Chloride, sulfate, TDS	1
M23	57.18	Poor	Chloride, sulfate, TDS	1
M24	63.01	Poor	Chloride, sulfate, TDS	1
M25	87.10	Very poor	Chloride, sulfate, Na	1

Note. WQI was calculated from pH, turbidity, TDS, total hardness, chloride, sulfate, sodium, iron, manganese, and zinc using the weights reported in Table 4. Quality categories were defined as excellent (WQI≤25), good (25<WQI≤50), poor (50<WQI≤75), very poor (75<WQI≤100), and unsuitable for drinking (WQI>100). The main contributing parameters are the three variables with the largest weighted sub-indices for each well. EC was excluded because TDS was derived from conductivity. Invariant elements and variables with unresolved analytical qualifiers were not included. Overall, 4 wells (16%) were classified as good, 7 (28%) as poor, 5 (20%) as very poor, and 9 (36%) as unsuitable; no well was classified as excellent. [1]The WQI for M11 was calculated using the recorded TDS value of 916 mg/L. This result remains provisional because the reported TDS is atypically low relative to its EC of 17,290 µS/cm.

3.8. Spatial patterns, management implications and study limitations

Spatial outputs represent measured groundwater-quality patterns and interpolated estimates rather than aquifer vulnerability or public-health risk. No DRASTIC or GALDIT assessment was conducted. DRASTIC requires depth to groundwater, recharge, aquifer material, soil characteristics, topography, vadose-zone properties, and hydraulic conductivity. GALDIT additionally considers groundwater level relative to sea level, distance from the coast, aquifer thickness, and validated evidence of saline intrusion (Guo et al., 2023). Figure 6 therefore presents measured exceedances within the sampling footprint.

The uneven distribution of the 25 wells also limits spatial interpretation. M2 and M3 share the same coordinates but have different depths, while M6–M7 and M20–M21 are closely spaced. Without screened-interval information, these differences cannot demonstrate vertical hydrochemical stratification. IDW assumes greater similarity among nearby locations but does not reproduce hydraulic boundaries, anisotropy, groundwater-flow paths, or aquifer geometry. Its performance should therefore be evaluated through cross-validation and prediction errors (Mukherjee & Singh, 2022).

M11 has the highest verification priority because it showed elevated salinity-related values, but its TDS of 916 mg/L is inconsistent with an EC of 17,290 µS/cm. M6–M8 require salinity review, whereas M12, M15, and M17 require confirmation of manganese concentrations and redox conditions. Management options include blending, desalination, manganese oxidation–filtration, improved drainage, controlled leaching, drip irrigation, and salt-tolerant crops. Managed aquifer recharge remains a potential option pending source-water testing, infiltration studies, clogging assessment, and long-term piezometric monitoring (Haritha et al., 2025).

There are many possible pressures that could be applied to the area in the lower Chira Valley. The highly irrigated agriculture, groundwater pumping, canals, sanitation problems, urban growth, livestock farming, and agricultural drainage fall under this category. Regional assessments indicate that the area is witnessing increased irrigated agriculture, salinity and drainage issues, improper water consumption, discharge of wastewater, rising demand, and the lack of continuous observation of groundwater (Consorcio ATA–UNP–UNL, 2005; ANA, 2015). This means that the mentioned conditions create a relevant context, but it does not imply any relevance between some environment and the specific activity.

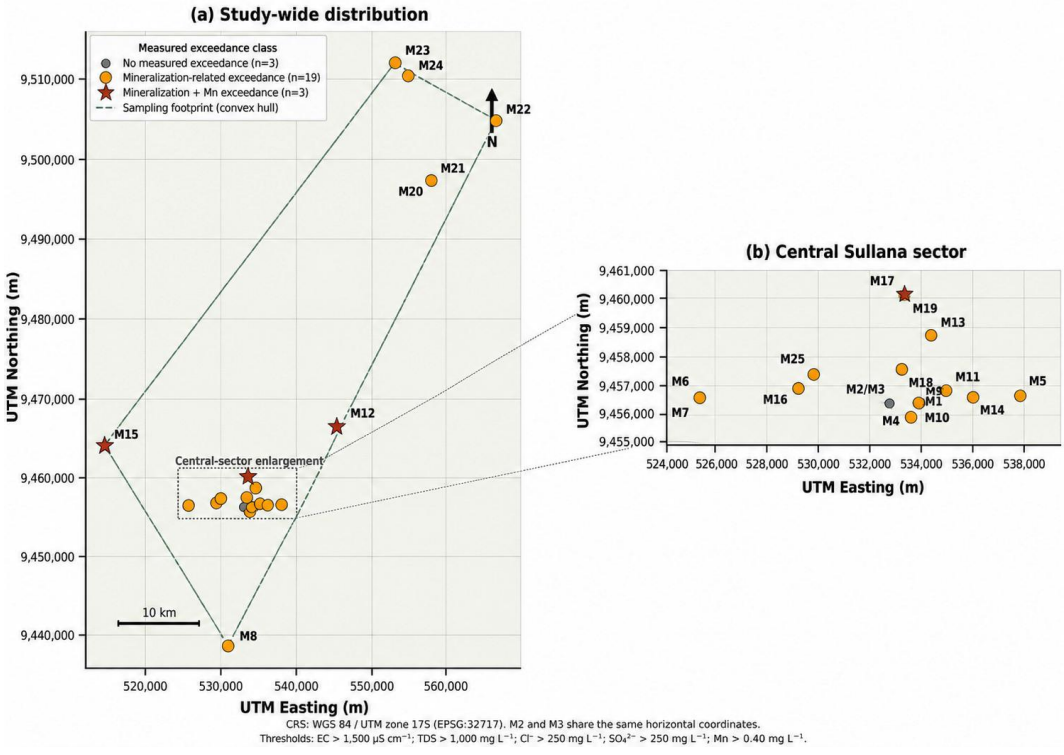


Figure 6. Spatial distribution of measured groundwater-quality exceedances in the Sullana study area. Note. Gray circles show no exceedance, orange circles mineralization, and red stars Mn exceedance. The dashed polygon marks the sampling footprint, not aquifer boundaries. M2–M3 share coordinates; observations do not indicate vulnerability or health risk.

The extraction of groundwater could change hydraulic gradients, create vertical mixing or move saline water from one point to another. Nevertheless, there is no information on pumping history, screening locations, seasonal groundwater levels, and hydraulic gradients. Future studies must use chemical and isotopic traces alongside well constructions, abstracts, methods, and data to ascertain the sources accurately. Human actions could enhance the natural processes of mineralization, but it has not been established yet how much they actually did so.

The groundwater characteristics in Sullana mirror those observed in the irrigated and semi-arid coastal aquifers where salinity can be caused by factors such as evaporation, mineral dissolution, cation exchange, irrigation return flow, seawater intrusion, and naturally saline water (Slama et al., 2022; Salman et al., 2024; Azari & Tabari, 2024). One significant regional example is found in the Peru–Chile Caplina–Concordia aquifer, where there have been significant interactions among river infiltration, irrigation return flow, side inflows, and marine intrusions, contributing to complex water chemistry that cannot be explained by traditional HCA (Narvaez-Montoya et al., 2024).

This study provides a dry-season baseline based on ionic ratios, Gibbs analysis, PCA, HCA, WQI, SAR, Na%, GIS interpolation, and parameter-specific exceedances. Interpretation is limited by a single campaign, 25 unevenly distributed wells, unknown screened intervals, unavailable groundwater levels, and the absence of pumping records. Seasonal studies show that hydrochemical facies, PCA loadings, clusters, WQI values, and salinity indicators may change following recharge or prolonged abstraction (Maman Hassan & Fırat Ersoy, 2022; Sadeghi-Lari et al., 2024; Ji et al., 2024; Pitchaimani et al., 2026).

The absence of validated HCO_3^-, CO_3^{2-}, Br^-, nitrogen species, microbial indicators, and stable isotopes prevented complete ionic-balance calculations and the application of anionic Gibbs, RSC, Revelle–Simpson, HFE-D, and PHREEQC analyses. Invariant trace-element values also require verification of LOD, LOQ, reporting qualifiers, blanks, certified-reference-material recoveries, and duplicate precision. Future research should include seasonal sampling, groundwater-level monitoring, verified screened intervals, abstraction inventories, end-member sampling, $\delta^{18}O$, $\delta^{2}H$, Cl^-/Br^-, and nitrate and sulfate isotopes (El Mountassir & Bahir, 2023; Zhang et al., 2023; Ji et al., 2024).

4. Conclusions

The research presents a comprehensive framework that assesses groundwater quality for the Sullana sector by integrating physicochemical characterization, ionic ratios, Gibbs relation for cations, principal component analysis, cluster analysis, weighted arithmetic water quality index, irrigation water indices, and spatial analysis methods. All of these make it possible to discern prevailing hydrochemical patterns as well as to distinguish the actual situation from interpolated estimates. However, it should be underlined that the obtained results refer only to one dry-season study and should be perceived not as what determines the seasonal behavior or trends in groundwater quality but rather as a spatial benchmark.

The principal finding is that groundwater-quality impairment is dominated by major-ion mineralization rather than uniform trace-metal contamination. PCA identified a broad mineralization component involving EC, TDS, Na^+, Cl^-, SO_4^{2-}, Ca^{2+}, and Mg^{2+}, whereas Fe and Mn showed a distinct variability pattern. Ionic ratios and the cationic Gibbs relationship support contributions from water–rock interaction, evaporation, mineral dissolution, ion exchange, and saline-water mixing. Nevertheless, the available evidence cannot definitively distinguish evaporite dissolution, irrigation return flow, inherited salinity, and contemporary seawater intrusion. Manganese represents a localized concern because three wells exceeded the national comparison value. In contrast, the invariant As, Pb, Cd, and Cu results require verification of their analytical qualifiers, LODs, LOQs, and reporting limits.

According to the WQI, the majority of the monitored cases posed considerable limitations for direct consumption as drinking-water sources. However, SAR, Na%, and electrical conductivity showed that the dangers of salinity and sodicity were not necessarily correlated. The management must focus on verifying M11 and checking manganese in M12, M15, and M17, then take care of the wells with the lowest mineral content and carry out seasonal observations of the most affected locations. In future programs, HCO_3^-, CO_3^{2-}, Br^-, nitrates, microbial indices, $\delta^{18}O$, $\delta^{2}H$, groundwater levels, screening intervals, and water extraction records should also be included. Sustainable management implies the need for joint regulation of the abstraction of groundwater resources, irrigation efficiency, drainage, and control of water quality.

Author contribution

H. Ore-Quiroz: Conceptualization, Methodology, Investigation, Data curation, Formal analysis, Visualization, Writing – original draft, Writing – review & editing. **C. Salazar-Sandoval:** Methodology, Validation, Formal analysis, Writing – review & editing. **E. Olaya-Ato:** Investigation, Data curation, Laboratory analysis, Writing – review & editing. **L. Camacho-Vidal:** Investigation, Data curation, Visualization, Writing – review & editing. **L. Espinoza-Haro:** Supervision, Validation, Writing – review & editing.

ORCID

H. Ore-Quiroz https://orcid.org/0000-0003-1649-7755
C. Salazar-Sandoval https://orcid.org/000-0002-9064-9609
E. Olaya-Ato https://orcid.org/0000-0001-9611-1407
L. Camacho-Vidal https://orcid.org/0000-0003-0888-4026
L. Espinoza-Haro https://orcid.org/0000-0002-5647-3312

References

Alexakis, D. E. (2022). Applying factor analysis and the CCME Water Quality Index for assessing groundwater quality of an Aegean Island, Rhodes, Greece. *Geosciences, 12*(10), 384. https://doi.org/10.3390/geosciences12100384

Alsabti, B., Sabarathinam, C., & Dhanu Radha, S. V. V. (2023). Identification of high nitrate concentration in shallow groundwater of an arid region: A case study of South Kuwait's Bay. *Environmental Monitoring and Assessment*, *195*, 143. https://doi.org/10.1007/s10661-022-10698-1

Appelo, C. A. J., & Postma, D. (2005). *Geochemistry, groundwater and pollution* (2nd ed.). CRC Press/Balkema.

Autoridad Nacional del Agua. (2015). Plan de gestión de los recursos hídricos de la cuenca Chira-Piura. Autoridad Nacional del Agua.

Araújo, A. M., dos Santos, L. L., Kozłowska, B., Walencik-Łata, A., de Aragão, R., de Paiva, W., Pereira Sousa, A. A., Silveira, T. N., Carvalho, A. K. N., Souza, E. S., dos Santos Filho, J. I., & Lalic, S. S. (2026). Integrated hydrochemical and radiological assessment of groundwater in the Seridó crystalline basement, Brazil: Evidence of geogenic influences on Ra and trace elements. *Journal of Environmental Radioactivity, 293*, 107877. https://doi.org/10.1016/j.jenvrad.2025.107877

Awasthi, A., Rishi, M. S., Khosla, A., & Panjgotra, S. (2023). Geographic information system-based groundwater quality assessment for drinking and irrigation purposes in transboundary aquifers of River Ravi, India. *Environmental Science and Pollution Research, 30*, 34536–34552. https://doi.org/10.1007/s11356-022-24642-w

Azari, T., & Tabari, M. M. R. (2024). An integrated approach based on HFE-D, GIS techniques, GQI-SWI, and statistical analysis for the assessment of potential seawater intrusion: Coastal multilayered aquifer of Ghaemshahr-Juybar, Mazandaran, Iran. *Environmental Science and Pollution Research, 31*, 13335–13371. https://doi.org/10.1007/s11356-024-31967-1

Benaafi, M., Abba, S. I., Tawabini, B., Abdulazeez, I., Salhi, B., Usman, J., & Aljundi, I. H. (2023). Integrated clustering analysis for delineating seawater intrusion and heavy metals in Arabian Gulf coastal groundwater of Saudi Arabia. *Heliyon, 9*, e19784. https://doi.org/10.1016/j.heliyon.2023.e19784

Cantwell, H. (Ed.). (2025). The fitness for purpose of analytical methods: A laboratory guide to method validation and related topics (3rd ed.). Eurachem.

Consorcio ATA–UNP–UNL. (2005). Caracterización hídrica y adecuación entre la oferta y la demanda en el ámbito de la cuenca binacional Catamayo-Chira. Proyecto Binacional Catamayo-Chira.

Dhakate, R. (2024). Characterization of groundwater salinity by hydrogeochemical and multivariate statistical analysis in the coastal aquifer of Nagapattinam District, Southern India. *Heliyon, 10*, e32396. https://doi.org/10.1016/j.heliyon.2024.e32396

Dougha, M., Selmane, T., Ahmed, A. A., Arafat, A. A., Ghoneim, S. S. M., Egbueri, J. C., Seraiche, L., & Hussein, E. E. (2026). A hybrid expert-PCA-ANN framework for hydrogeochemical optimization of the Water Quality Index in a semi-arid aquifer. *Physics and Chemistry of the Earth, 144*, 104657. https://doi.org/10.1016/j.pce.2026.104657

El Mountassir, O., & Bahir, M. (2023). The assessment of groundwater quality in the coastal aquifers of the Essaouira Basin, southwestern Morocco, using hydrogeochemistry and isotopic signatures. *Water, 15*, 1769. https://doi.org/10.3390/w15091769

Gomes, L. A., Barbosa, N. S., Debruyne, D., Barbosa, N., Moitinho, D. E. R., Peixoto, R., Santos, C. B., & Peixinho, M. A. L. (2023). Hydrogeochemical processes and groundwater evolution of the São Sebastião-Marizal aquifer system in the Tucano Central Basin, Bahia, Brazil. *Journal of South American Earth Sciences, 127*, 104413. https://doi.org/10.1016/j.jsames.2023.104413

Guo, X., Yang, Z., Li, C., Xiong, H., & Ma, C. (2023). Combining the classic vulnerability index and affinity propagation clustering algorithm to assess the intrinsic aquifer vulnerability of coastal aquifers on an integrated scale. *Environmental Research, 217*, 114877. https://doi.org/10.1016/j.envres.2022.114877

Ha, Q. K., Tran, B. L., & Lai, V. Q. (2026). Groundwater salinization and anthropogenic pollution imprints revealed by unsupervised learning in Ho Chi Minh City. Groundwater for Sustainable Development, 33, 101589. https://doi.org/10.1016/j.gsd.2026.101589

Hamma, B., Bekkouche, M. F., Bouaicha, F., Elnagdy, K. A., Alzaed, A., Barkat, A., Randazzo, A., Andualem, M. S., & Hussein, E. E. (2025). Hydrogeochemical assessment of groundwater for agricultural suitability in the Ksour Mountains, Algeria. *Scientific Reports, 15*, 36441. https://doi.org/10.1038/s41598-025-20352-8

Haritha, V. K., Raicy, M. C., & Elango, L. (2025). Enhancing groundwater quality in a saline coastal aquifer through managed aquifer recharge: A comprehensive study by long-term groundwater level and hydrochemical monitoring. *Groundwater for Sustainable Development, 30*, 101480. https://doi.org/10.1016/j.gsd.2025.101480

Hou, Z., Huang, L., Zhang, S., Han, X., Xu, J., & Li, Y. (2024). Identification of groundwater hydrogeochemistry and the hydraulic connections of aquifers in a complex coal mine. *Journal of Hydrology, 628*, 130496. https://doi.org/10.1016/j.jhydrol.2023.130496

International Organization for Standardization. (2009). ISO 5667-11:2009: Water quality: Sampling: Part 11: Guidance on sampling of groundwaters. ISO.

International Organization for Standardization. (2017). ISO/IEC 17025:2017: General requirements for the competence of testing and calibration laboratories. ISO.

International Organization for Standardization. (2024). ISO 5667-3:2024: Water quality: Sampling: Part 3: Preservation and handling of water samples. ISO.

Ji, D., Ma, J., Xue, J., Wu, X., Wang, Z., & Wei, S. (2024). Identifying groundwater characteristics and controlling factors in Jiaozhou Bay's northern coastal region, China: A combined approach of multivariate statistics, isotope analysis, and field empirical investigations. *Scientific Reports, 14*, 23856. https://doi.org/10.1038/s41598-024-75425-x

Jiang, L., Sui, H., Kang, F., Li, C., Wei, S., Yu, L., & Li, Y. (2023). Hydrogeochemical characteristics and formation mechanism of the karst thermal reservoir at the northern edge of the Luzhong Uplift. *Carsologica Sinica, 42*(5), 1005–1026. https://doi.org/10.11932/karst20230514

Liang, C.-P., Lin, T.-C., Suk, H., Wang, C.-H., Liu, C.-W., Chang, T.-W., & Chen, J.-S. (2022). Comprehensive assessment of the impact of land use and hydrogeological properties on

groundwater quality in Taiwan using factor and cluster analyses. *Science of the Total Environment*, *851*, 158135. https://doi.org/10.1016/j.scitotenv.2022.158135

Lipps, W. C., Braun-Howland, E. B., & Baxter, T. E. (Eds.). (2023). Standard methods for the examination of water and wastewater (24th ed.). APHA Press.

Maman Hassan, A., & Fırat Ersoy, A. (2022). Statistical assessment of seasonal variation of groundwater quality in Çarşamba coastal plain, Samsun, Turkey. *Environmental Monitoring and Assessment*, *194*, 135. https://doi.org/10.1007/s10661-022-09791-2

Manu, E., Loh, Y. S. A., Obiri-Nyarko, F., Afrifa, G. Y., & Karikari, A. Y. (2026). Groundwater quality and hydrogeochemical controls in crystalline basement and Neoproterozoic Voltaian sedimentary aquifers of central Ghana. *Groundwater for Sustainable Development*, *34*, 101656. https://doi.org/10.1016/j.gsd.2026.101656

Mêlo, F. E. L. de, Peixoto, F. da S., Morais, C. C. de O., Gomes, M. da C. R., & Dias, G. H. (2023). Coastal aquifer water quality for domestic supply of small communities in the semiarid Potiguar, Brazilian Northeast. *Journal of South American Earth Sciences*, *132*, 104633. https://doi.org/10.1016/j.jsames.2023.104633

Mester, T., Szabó, G., Kiss, E., & Balla, D. (2026). Hydrochemical assessment of shallow groundwater in a rural settlement following sewerage network development. *Water*, *18*, 1559. https://doi.org/10.3390/w18131559

Ministerio de Salud. (2010). Reglamento de la calidad del agua para consumo humano: Decreto Supremo N.° 031-2010-SA. Dirección General de Salud Ambiental, Ministerio de Salud del Perú.

Ministerio del Ambiente. (2017). Decreto Supremo N.° 004-2017-MINAM: Aprueban Estándares de Calidad Ambiental para Agua y establecen disposiciones complementarias. Ministerio del Ambiente del Perú.

Missaoui, R., Gentilucci, M., Hamed, Y., Hadji, R., Bouri, S., & Pambianchi, G. (2026). Irrigation-driven groundwater recharge and quality degradation in semi-arid regions: Hydrochemical, GIS-based, and explainable machine learning assessment in Central Tunisia. *Applied Sciences*, *16*, 7014. https://doi.org/10.3390/app16147014

Mukherjee, I., & Singh, U. K. (2022). Hydrogeochemical characterizations and quality evaluation of groundwater in the major river basins of a geologically and anthropogenically driven semi-arid tract of India. *Science of the Total Environment*, *805*, 150323. https://doi.org/10.1016/j.scitotenv.2021.150323

Narvaez-Montoya, C., Mahlknecht, J., Torres-Martínez, J. A., Mora, A., & Pino-Vargas, E. (2024). FlowSOM clustering: A novel pattern recognition approach for water research: Application to a hyper-arid coastal aquifer system. *Science of the Total Environment*, *915*, 169988. https://doi.org/10.1016/j.scitotenv.2024.169988

Nefla, L., Bergal, A., Boumaraf, W., Soukeur, A., Abukhadra, M. R., Bin-Jumah, M., Allam, A. A., Mikita, V., Szűcs, P., & Eid, M. H. (2026). Severe groundwater contamination in an industrialized coastal aquifer of northeastern Algeria: Integrated hydrogeochemical characterization and assessment of environmental and human health risks. *Journal of Hydrology: Regional Studies*, *67*, 103833. https://doi.org/10.1016/j.ejrh.2026.103833

Ohmer, M., Liesch, T., Goeppert, N., & Goldscheider, N. (2019). On the optimal selection of interpolation methods for groundwater-quality mapping. *Hydrogeology Journal*, *27*, 2901–2918. https://doi.org/10.1007/s10040-019-02028-4

Omena, A. L., Ihimekpen, N. I., & Okonofua, S. E. (2025). Principal component analysis of hydrochemical parameters in hydrocarbon-affected groundwater at Otorogu, Delta State, Nigeria. *Nigerian Journal of Environmental Sciences and Technology*, *9*(2), 149–163. https://doi.org/10.36263/nijest.2025.02.63

Pitchaimani, V. S., Aswin, S. K., Sidhu, N., Sharma, S., Promilton, A. A. A., Abishek, R. A. S., & Joe, R. J. J. (2026). Seasonal hydrogeochemical signatures of seawater intrusion and salinity stress in a coastal aquifer system of southern Tamil Nadu, India. *Journal of Trace Elements and Minerals*, *18*, 100324. https://doi.org/10.1016/j.jtemin.2026.100324

Proyecto Especial Chira Piura. (2021, 16 de agosto). *Nota de prensa: El PECHP informa*. Plataforma Digital Única del Estado Peruano. https://www.gob.pe/institucion/pechp/noticias/623998-nota-de-prensa-el-pechp-informa

Sadeghi-Lari, A., Bahrami, M., & Dastandaz, T. (2024). Temporal and spatial variations of groundwater quantity and quality for drinking and irrigation purposes in the arid and hot weather of Southern Iran. *Physics and Chemistry of the Earth*, *134*, 103582. https://doi.org/10.1016/j.pce.2024.103582

Salman, S. A., Abou El-Anwar, E. A., Aita, S. K., & Elnazer, A. A. (2024). Geo-environmental factors controlling groundwater hydrogeochemistry, salinization and quality in El Qaa Plain coastal aquifer, Southwest Sinai, Egypt. *Environment, Development and Sustainability*, *26*, 28591–28609. https://doi.org/10.1007/s10668-023-03830-9

Sanad, H., Moussadek, R., Zouahri, A., Oueld Lhaj, M., Mouhir, L., & Dakak, H. (2025). Machine learning-integrated hydrogeochemical and spatial modeling of groundwater quality indices for seawater intrusion and irrigation sustainability in coastal agroecosystems of Skhirat Region, Morocco. *Journal of Hydrology: Regional Studies*, *62*, Article 102848. https://doi.org/10.1016/j.ejrh.2025.102848

Slama, F., Nasri, N., & Bouhlila, R. (2022). Delineating the origins and processes of groundwater salinization and quality degradation in a coastal irrigated plain, Korba, northeastern Tunisia. *Marine Pollution Bulletin*, *181*, 113914. https://doi.org/10.1016/j.marpolbul.2022.113914

Sugumaran, S., Kulandaisamy, P., Rajendran, M., Karthikeyan, S., Senapathi, V., Thangaraj, K., & Ramanathan, S. (2026). Heavy metal behavior in semi-arid groundwater systems of Tiruchirappalli, Tamil Nadu: Environmental insights. *Water, Air, & Soil Pollution*, *237*, 539. https://doi.org/10.1007/s11270-026-09193-x

Tziritis, E., Sachsamanoglou, E., & Güler, C. (2024). Evaluating spatiotemporal groundwater quality changes in the Rhodope coastal aquifer system, NE Greece, employing a GIS-assisted hybrid approach of multivariate statistics and inverse geochemical modeling. *Science of the Total Environment*, *947*, 174676. https://doi.org/10.1016/j.scitotenv.2024.174676

Voutchkova, D. D., Ernstsen, V., Schullehner, J., Hinsby, K., Thorling, L., & Hansen, B. (2021). Roadmap for determining natural background levels of trace metals in groundwater. *Water*, *13*(9), 1267. https://doi.org/10.3390/w13091267

Wang, Y., Yin, Z., Sun, X., Zheng, E., Pan, J., Wu, J., & Wu, J. (2026). From sources to risks: A multi-method approach to groundwater hydrogeochemical evolution in the Hotan Oasis of an arid inland river basin, Northwest China. *Journal of Hydrology*, *675*, 135641. https://doi.org/10.1016/j.jhydrol.2026.135641

WHO (World Health Organization). (2026). Guidelines for drinking-water quality: Fourth edition incorporating the first, second and third addenda. World Health Organization.

Wurl, J., Imaz-Lamadrid, M. A., Mendez-Rodriguez, L. C., & Hernández-Morales, P. (2023). Hydrochemical indicator analysis of seawater intrusion into coastal aquifers of semiarid areas. *Resources*, *12*(4), 47. https://doi.org/10.3390/resources12040047

Ximenes, M., Pratas, J. A. M. S., De Azevedo, J. M. M., Figueiredo, F. P. O. O., & Currell, M. (2026). Identification of hydrochemical processes and assessment of groundwater quality: A case study of the intergranular aquifer in Dili City,

Timor-Leste. *Geology, Ecology, and Landscapes*, *10*(1), 238–260. https://doi.org/10.1080/24749508.2025.2449622

Zeng, Y., Wu, Q., Mei, A., Wang, L., Yin, W., Yang, L., Zhao, D., Meng, S., & Gao, H. (2024). Hydrogeochemical process and coal mining-motivated effect on hydrochemistry of the groundwater system in a mining area of Western China. *Journal of Geochemical Exploration*, *263*, 107516. https://doi.org/10.1016/j.gexplo.2024.107516

Zhang, C., Li, X., Wang, Z., Hou, X., Ma, J., Gao, M., Bai, Z., Fu, C., Gui, C., & Zuo, X. (2023). Combining stable isotopes (^{2}H,^{18}O, and $^{87}Sr/^{86}Sr$) and hydrochemistryto understand hydrogeochemical processes in a karst groundwater system, Xin'an, northern China. *Environmental Earth Sciences*, *82*, 224. https://doi.org/10.1007/s12665-023-10906-2

Zhi, C., Cao, W., Wang, Z., Li, Z., & Ren, Y. (2022). Genesis of As in groundwater with extremely high salinity in the Yellow River Delta, China. *Applied Geochemistry*, *139*, 105229. https://doi.org/10.1016/j.apgeochem.2022.105229

Zhou, J., Wu, Q., Gao, S., Zhang, X., Wang, Z., Wu, P., & Zeng, J. (2023). Coupled controls of river infiltration, urban activities, and carbonate on trace elements in a karst groundwater system from Guiyang, Southwest China. *Ecotoxicology and Environmental Safety*, *249*, 114424. https://doi.org/10.1016/j.ecoenv.2022.114424